

# A structure-preserving parametric finite element method for geometric flows with anisotropic surface energy

Weizhu Bao · Yifei Li

Received: date / Accepted: date

**Abstract** We propose and analyze structure-preserving parametric finite element methods (SP-PFEM) for evolution of a closed curve under different geometric flows with arbitrary anisotropic surface energy  $\gamma(\mathbf{n})$  for  $\mathbf{n} \in \mathbb{S}^1$  representing the outward unit normal vector. By introducing a novel surface energy matrix  $\mathbf{G}_k(\mathbf{n})$  depending on  $\gamma(\mathbf{n})$  and the Cahn-Hoffman  $\xi$ -vector as well as a nonnegative stabilizing function  $k(\mathbf{n}) : \mathbb{S}^1 \rightarrow \mathbb{R}$ , which is a sum of a symmetric positive definite matrix and an anti-symmetric matrix, we obtain a new geometric partial differential equation and its corresponding variational formulation for the evolution of a closed curve under anisotropic surface diffusion. Based on the new weak formulation, we propose a parametric finite element method for the anisotropic surface diffusion and show that it is area conservation and energy dissipation under a very mild condition on  $\gamma(\mathbf{n})$ . The SP-PFEM is then extended to simulate evolution of a close curve under other anisotropic geometric flows including anisotropic curvature flow and area-conserved anisotropic curvature flow. Extensive numerical results are reported to demonstrate the efficiency and unconditional energy stability as well as good mesh quality property of the proposed SP-PFEM for simulating anisotropic geometric flows.

**Keywords** geometric flows · parametric finite element method · anisotropy surface energy · structure-preserving · area conservation · energy-stable

**Mathematics Subject Classification (2000)** 65M60, 65M12, 35K55, 53C44

---

W. Bao  
Department of Mathematics, National University of Singapore, Singapore 119076  
Fax: +65-6779-5452, Tel.: +65-6516-2765,  
URL: <https://blog.nus.edu.sg/matbwz/>  
E-mail: matbaowz@nus.edu.sg

Y. Li  
Department of Mathematics, National University of Singapore, Singapore 119076  
E-mail: e0444158@u.nus.edu

## 1 Introduction

Anisotropic surface energy along surface/interface is ubiquitous in solids and materials science due to the lattice orientational difference [15, 26]. It thus generates anisotropic evolution process of interface/surface (or geometric flows with anisotropic surface energy) in material sciences [28, 36, 39], imaging sciences [18, 21, 33], and computational geometry [15, 19, 40]. In fact, anisotropic geometric flows have significant and broader applications in materials science, solid-state physics and computational geometry, such as grain boundary growth [12], foam bubble/film [35], surface phase formation [44], epitaxial growth [24, 26], heterogeneous catalysis [34], solid-state dewetting [4, 6, 39], computational graphics [18, 21, 33].

Assume  $\Gamma$  be a closed curve in two dimensions (2D) associated with a given anisotropic surface energy  $\gamma(\mathbf{n})$ , where  $\mathbf{n} = (n_1, n_2)^T \in \mathbb{S}^1$  representing the unit outward normal vector, and define the free energy functional of the closed curve  $\Gamma$  associate with anisotropic surface energy  $\gamma(\mathbf{n})$  as

$$W(\Gamma) := \int_{\Gamma} \gamma(\mathbf{n}) ds, \quad (1.1)$$

where  $s$  denotes the arc-length parameter of  $\Gamma$ . By applying the thermodynamic variation, one can obtain the chemical potential  $\mu := \mu(s)$  (or weighted curvature denoted as  $\kappa_{\gamma} := \kappa_{\gamma}(s)$ ) generated from the energy functional  $W(\Gamma)$  as [30, 37]

$$\mu = \kappa_{\gamma} := \frac{\delta W(\Gamma)}{\delta \Gamma} = \lim_{\varepsilon \rightarrow 0} \frac{W(\Gamma^{\varepsilon}) - W(\Gamma)}{\varepsilon}, \quad (1.2)$$

where  $\Gamma^{\varepsilon}$  is a small perturbation of  $\Gamma$ . Different geometric flows associate with the anisotropic surface energy  $\gamma(\mathbf{n})$  can be easily defined by providing the normal velocity  $V_n$  for evolution of  $\Gamma$ . Typical geometric flows widely used in different applications including anisotropic curvature flow, area-conserved anisotropic curvature flow and anisotropic surface diffusion with the corresponding normal velocity  $V_n$  given as [1, 13, 14, 17, 38]

$$V_n = \begin{cases} -\mu, & \text{anisotropic curvature flow,} \\ -\mu + \lambda, & \text{area-conserved anisotropic curvature flow,} \\ \partial_{ss}\mu, & \text{anisotropic surface diffusion,} \end{cases} \quad (1.3)$$

where  $\lambda$  is chosen such that the area of the region enclosed by  $\Gamma$  is conserved, which is given as

$$\lambda = \frac{\int_{\Gamma} \mu ds}{\int_{\Gamma} 1 ds}, \quad \Leftrightarrow \quad \int_{\Gamma} V_n ds = \int_{\Gamma} (-\mu + \lambda) ds = 0. \quad (1.4)$$

We remark here that if  $\gamma(\mathbf{n}) \equiv 1$  for  $\mathbf{n} \in \mathbb{S}^1$ , i.e. isotropic surface energy, then the chemical potential defined in (1.2) collapses to the curvature  $\kappa$  of  $\Gamma$ , and then the geometric flows defined in (1.3) collapse to curvature flow (or curve-shortening flow), area-conserved curvature flow and surface diffusion, respectively, we refer to the review paper [13].

Based on different parametrizations of  $\Gamma$  and mathematical formulations for the geometric flows (1.3), several numerical methods have been proposed for simulating

the geometric flows (1.3) with isotropic and anisotropic surface energy corresponding to  $\gamma(\mathbf{n}) \equiv 1$  and  $\gamma(\mathbf{n}) \neq \text{const}$ , respectively. These numerical methods include the level set method and the phase-field method [23], the marker particle method [22, 42], the finite element method based on graph formulation [19, 20], the discontinuous Galerkin method [43], the crystalline method [16, 25], the evolving surface finite element method (ESFEM) [31], and the parametric finite element method (PFEM) [8, 10]. Due to that only the normal velocity is given in the anisotropic geometric flows (1.3), different artificial tangential velocities are introduced in different numerical methods, which cause different accuracies and mesh qualities, and thus some methods need to carry out re-mesh frequently during evolution to avoid the collision of mesh points. Among those numerical methods, the PFEM proposed by Barrett, Garcke, and Nürnberg (also called as BGN scheme in the literature) demonstrates several good properties including efficiency and accuracy, unconditional energy stability and asymptotic equal-mesh distribution for isotropic geometric flows. Recently, by introducing a clever approximation of the normal vector, Bao and Zhao proposed a structure-preserving PFEM (SP-PFEM) [2, 7] for surface diffusion. Different techniques have been proposed to extend PFEM or SP-PFEM for isotropic geometric flows to anisotropic geometric flows in the literatures [9, 11, 29, 30, 32, 40]. Very recently, by introducing a symmetric positive definite surface matrix  $\mathbf{Z}_k(\mathbf{n})$  depending on  $\gamma(\mathbf{n})$  and the Cahn-Hoffman  $\boldsymbol{\xi}$ -vector as well as a stabilizing function  $k(\mathbf{n}) : \mathbb{S}^1 \rightarrow \mathbb{R}^+$  [3, 5], we successfully and systematically extended the SP-PFEM method from isotropic surface diffusion to anisotropic surface diffusion under a symmetric (and necessary) condition on  $\gamma(\mathbf{n})$  as:  $\gamma(\mathbf{n}) = \gamma(-\mathbf{n})$  for  $\mathbf{n} \in \mathbb{S}^1$ . Unfortunately, there are different anisotropic surface energy  $\gamma(\mathbf{n})$  which is not symmetric, e.g. the 3-fold anisotropic surface energy [4, 40], in different applications. Thus the proposed SP-PFEM in [3, 5] cannot be applied to handle anisotropic geometric flows with non-symmetric surface energy  $\gamma(\mathbf{n})$ .

In fact, it is still open to design a structure-preserving parametric finite element method (SP-PFEM) for anisotropic geometric flows (1.3) with general anisotropy  $\gamma(\mathbf{n})$ , especially when  $\gamma(\mathbf{n}) \neq \gamma(-\mathbf{n})$ . The main aim of this paper is to attack this important and challenging problem. The main ingredients in the proposed methods are based on: (i) the introduction of a novel surface energy matrix  $\mathbf{G}_k(\mathbf{n})$  depending on  $\gamma(\mathbf{n})$  and the Cahn-Hoffman  $\boldsymbol{\xi}$ -vector as well as a stabilizing function  $k(\mathbf{n}) : \mathbb{S}^1 \rightarrow \mathbb{R}^+$ , which can be explicitly decoupled into a symmetric positive definite matrix and an anti-symmetric matrix, (ii) a new conservative geometric partial differential equation (PDE), (iii) a new variational formulation, and (iv) a proper approximation of the normal vector. We prove that the proposed SP-PFEM is structure-preserving, i.e. area conservation and energy dissipation, for anisotropic surface diffusion under a very mild condition

$$3\gamma(\mathbf{n}) > \gamma(-\mathbf{n}), \quad \mathbf{n} \in \mathbb{S}^1. \quad (1.5)$$

Finally we extend the proposed SP-PFEM to simulate evolution of a closed curve under other anisotropic geometric flows including anisotropic curvature flow and area-conserved anisotropic curvature flow.

The remainder of this paper is organized as follows: In section 2, by introducing the surface energy matrix  $\mathbf{G}_k(\mathbf{n})$ , we derive a new conservative PDE and its corresponding variational formulation for anisotropic surface diffusion, and propose

the semi-discretization in space and the full-discretization by SP-PFEM. In section 3, we establish the unconditional energy dissipation of the proposed SP-PFEM for anisotropic surface diffusion. In section 4, we extend the proposed SP-PFEM to the anisotropic curvature flow and area-conserved anisotropic curvature flow. Extensive numerical results are reported in section 5 to illustrate the efficiency and accuracy as well as structure-preserving properties of the proposed SP-PFEM. Finally, some concluding remarks are drawn in section 6.

## 2 The structure-preserving PFEM for anisotropic surface diffusion

In this section, by taking the anisotropic surface diffusion in (1.3), we introduce a surface energy matrix  $\mathbf{G}_k(\mathbf{n})$ , obtain a conservative geometric PDE and derive its corresponding variational formulation. An SP-PFEM for the variational problem is presented and its structural-preserving property is stated under a very mild condition on the anisotropic surface energy  $\gamma(\mathbf{n})$ .

### 2.1 The geometric PDE

Let  $\Gamma := \Gamma(t)$  be parameterized by  $\mathbf{X} := \mathbf{X}(s, t) = (x(s, t), y(s, t))^T \in \mathbb{R}^2$  with  $s$  denoting the time-dependent arc-length parametrization (or ‘Lagrangian coordinate’) of  $\Gamma$  and  $t$  representing the time. Then the anisotropic surface diffusion of  $\Gamma$  can be described by

$$\partial_t \mathbf{X} = \partial_{ss} \mu \mathbf{n}, \quad (2.1)$$

where  $\mathbf{n} = (n_1, n_2)^T \in \mathbb{S}^1$  represents the unit outward normal vector of  $\Gamma$ . In practice, another popular way (or ‘Eulerian coordinate’) is to adopt  $\rho \in \mathbb{T} = \mathbb{R}/\mathbb{Z} = [0, 1]$  being the periodic interval and then parameterize  $\Gamma(t)$  on  $\mathbb{T}$  by  $\mathbf{X}(\rho, t)$ , which is given as

$$\Gamma(t) := \mathbf{X}(\cdot, t) \quad \mathbf{X}(\cdot, t) : \mathbb{T} \rightarrow \mathbb{R}^2, (\rho, t) \mapsto (x(\rho, t), y(\rho, t))^T. \quad (2.2)$$

Then the arc-length parameter  $s$  is given as  $s(\rho, t) = \int_0^\rho |\partial_\rho \mathbf{X}(\rho, t)| d\rho$  satisfying  $\partial_\rho s = |\partial_\rho \mathbf{X}|$ . We assume that the parametrization by  $\rho$  is regular during the evolution, i.e., there is a constant  $C > 1$  such that  $\frac{1}{C} \leq |\partial_\rho s(\rho, t)| \leq C$ . The normal velocity  $V_n$  can be given by this parametrization as

$$V_n = \mathbf{n} \cdot \partial_t \mathbf{X}. \quad (2.3)$$

In order to get an explicit formula of  $\mu$  from  $\gamma(\mathbf{n})$ , let  $\gamma(\mathbf{p})$  be a one-homogeneous extension of  $\gamma(\mathbf{n})$  from  $\mathbb{S}^1$  to  $\mathbb{R}^2$ , e.g.

$$\gamma(\mathbf{p}) := \begin{cases} |\mathbf{p}| \gamma\left(\frac{\mathbf{p}}{|\mathbf{p}|}\right), & \forall \mathbf{p} = (p_1, p_2)^T \in \mathbb{R}_*^2 := \mathbb{R}^2 \setminus \{\mathbf{0}\}, \\ 0, & \mathbf{p} = \mathbf{0}, \end{cases} \quad (2.4)$$

where  $|\mathbf{p}| = \sqrt{p_1^2 + p_2^2}$ . Based on this homogeneous extension  $\gamma(\mathbf{p})$ , we can talk the regularity of  $\gamma(\mathbf{n})$  by referring to the regularity of  $\gamma(\mathbf{p})$ , i.e.,  $\gamma(\mathbf{n}) \in C^2(\mathbb{S}^1) \iff \gamma(\mathbf{p}) \in C^2(\mathbb{R}^2 \setminus \{\mathbf{0}\})$ . Then we introduce the Cahn-Hoffman  $\boldsymbol{\xi}$ -vector [27, 41] as

$$\boldsymbol{\xi} := \boldsymbol{\xi}(\mathbf{n}) : \mathbb{S}^1 \rightarrow \mathbb{R}^2, \quad \mathbf{n} \mapsto \boldsymbol{\xi} = (\xi_1, \xi_2)^T := \nabla \gamma(\mathbf{p})|_{\mathbf{p}=\mathbf{n}} = \gamma(\mathbf{n}) \mathbf{n} + (\boldsymbol{\xi} \cdot \boldsymbol{\tau}) \boldsymbol{\tau}, \quad (2.5)$$

here  $\boldsymbol{\tau} = \partial_s \mathbf{X} = \mathbf{n}^\perp$  is the unit tangential vector of  $\Gamma$ , and  $\perp$  denoting the clockwise rotation by  $\frac{\pi}{2}$ . Then an explicit formulation of  $\mu$  can be expressed as the  $\boldsymbol{\xi}$ -vector as [30]

$$\mu := \mu(\mathbf{n}) = -\mathbf{n} \cdot \partial_s \boldsymbol{\xi}^\perp. \quad (2.6)$$

Thus another equivalent geometric PDE for anisotropic surface diffusion can be given as

$$\mathbf{n} \cdot \partial_t \mathbf{X} = \partial_{ss} \mu, \quad (2.7a)$$

$$\mu = -\mathbf{n} \cdot \partial_s \boldsymbol{\xi}^\perp, \quad \boldsymbol{\xi}(\mathbf{n}) = \nabla \gamma(\mathbf{p})|_{\mathbf{p}=\mathbf{n}}. \quad (2.7b)$$

## 2.2 The surface energy matrix

Introduce the surface energy matrix  $\mathbf{G}_k(\mathbf{n})$  as

$$\mathbf{G}_k(\mathbf{n}) := \gamma(\mathbf{n})I_2 - \mathbf{n}\boldsymbol{\xi}^T + \boldsymbol{\xi}\mathbf{n}^T + k(\mathbf{n})\mathbf{n}\mathbf{n}^T := \mathbf{G}_k^{(s)}(\mathbf{n}) + \mathbf{G}^{(a)}(\mathbf{n}), \quad \forall \mathbf{n} \in \mathbb{S}^1, \quad (2.8)$$

where  $I_2$  is the  $2 \times 2$  identity matrix,  $k(\mathbf{n}) : \mathbb{S}^1 \rightarrow \mathbb{R}$  is a nonnegative stabilizing function to be determined later, and  $\mathbf{G}_k^{(s)}(\mathbf{n})$  and  $\mathbf{G}^{(a)}(\mathbf{n})$  are a symmetric positive matrix and an anti-symmetric matrix, respectively, which are given as

$$\mathbf{G}_k^{(s)}(\mathbf{n}) := \gamma(\mathbf{n})I_2 + k(\mathbf{n})\mathbf{n}\mathbf{n}^T, \quad \mathbf{G}^{(a)}(\mathbf{n}) := -\mathbf{n}\boldsymbol{\xi}^T + \boldsymbol{\xi}\mathbf{n}^T, \quad \forall \mathbf{n} \in \mathbb{S}^1. \quad (2.9)$$

Then we get the relationship between the weighted curvature  $\mu$  and the newly constructed  $\mathbf{G}_k(\mathbf{n})$  as

**Lemma 2.1** *The weighted curvature  $\mu$  defined in (2.6) has the following alternative explicit expression*

$$\mu \mathbf{n} = -\partial_s (\mathbf{G}_k(\mathbf{n}) \partial_s \mathbf{X}). \quad (2.10)$$

*Proof* From [3, Lemma 2.1], we know that

$$\mu \mathbf{n} = -\partial_s \boldsymbol{\xi}^\perp, \quad \boldsymbol{\xi}^\perp = \gamma(\mathbf{n})\boldsymbol{\tau} - (\boldsymbol{\xi} \cdot \boldsymbol{\tau})\mathbf{n}. \quad (2.11)$$

Thus it suffices to show  $\mathbf{G}_k(\mathbf{n}) \partial_s \mathbf{X} = \boldsymbol{\xi}^\perp$ . Since  $\partial_s \mathbf{X} = \boldsymbol{\tau}$ , by using the definition of  $\mathbf{G}_k(\mathbf{n})$  in (2.8), we can simplify  $\mathbf{G}_k(\mathbf{n}) \partial_s \mathbf{X}$  as

$$\begin{aligned} \mathbf{G}_k(\mathbf{n}) \partial_s \mathbf{X} &= \mathbf{G}_k(\mathbf{n}) \boldsymbol{\tau} = (\gamma(\mathbf{n})I_2 - \mathbf{n}\boldsymbol{\xi}^T + \boldsymbol{\xi}\mathbf{n}^T + k(\mathbf{n})\mathbf{n}\mathbf{n}^T) \boldsymbol{\tau} \\ &= \gamma(\mathbf{n})\boldsymbol{\tau} - (\boldsymbol{\xi} \cdot \boldsymbol{\tau})\mathbf{n} + (\mathbf{n} \cdot \boldsymbol{\tau})\boldsymbol{\xi} + k(\mathbf{n})(\mathbf{n} \cdot \boldsymbol{\tau})\mathbf{n} \\ &= \gamma(\mathbf{n})\boldsymbol{\tau} - (\boldsymbol{\xi} \cdot \boldsymbol{\tau})\mathbf{n} = \boldsymbol{\xi}^\perp. \end{aligned} \quad (2.12)$$

Combining (2.12) and (2.11), we get the desired equality (2.10).  $\square$

*Remark 2.1* The surface energy matrix  $\mathbf{G}_k(\mathbf{n})$  given here can not be symmetric unless  $\mathbf{n}\boldsymbol{\xi}^T = \boldsymbol{\xi}\mathbf{n}^T$ , which implies  $\gamma(\mathbf{n})\mathbf{n} = \mathbf{n}\boldsymbol{\xi}^T \mathbf{n} = \boldsymbol{\xi}\mathbf{n}^T = \boldsymbol{\xi}$ . This can only happen when  $\gamma(\mathbf{n})$  is isotropic. For anisotropic  $\gamma(\mathbf{n})$ ,  $\mathbf{G}_k(\mathbf{n})$  is essentially different from the symmetric surface energy matrix  $Z_k(\mathbf{n})$  introduced in [3, 5]. Moreover, if we choose  $k(\mathbf{n})$  to be 0, then  $\mathbf{G}_0(\mathbf{n})$  will collapse to the surface energy matrix  $G(\theta)$  given in [32]. This fact also means different from the stabilizing function in [3], in this paper we do not need the stabilizing function  $k(\mathbf{n})$  to be strictly positive.

By applying (2.10), the geometric PDE for anisotropic surface diffusion (2.7) can be rewritten as the following *conservative form*

$$\mathbf{n} \cdot \partial_t \mathbf{X} = \partial_{ss} \mu, \quad (2.13a)$$

$$\mu \mathbf{n} = -\partial_s (\mathbf{G}_k(\mathbf{n}) \partial_s \mathbf{X}). \quad (2.13b)$$

### 2.3 A variational formulation and its properties

We then derive the variational formulation for the conservative form (2.13). The functional space with respect to  $\Gamma(t)$  can be given as

$$L^2(\mathbb{T}) := \left\{ u : \mathbb{T} \rightarrow \mathbb{R} \mid \int_{\mathbb{T}} |u(\rho)|^2 d\rho < \infty \right\}, \quad (2.14)$$

with the following weighted  $L^2$ -inner product  $(\cdot, \cdot)_{\Gamma(t)}$

$$(u, v)_{\Gamma(t)} := \int_{\Gamma(t)} u(s)v(s)ds = \int_{\mathbb{T}} u(\rho)v(\rho)\partial_\rho s(\rho, t) d\rho, \quad \forall u, v \in L^2(\mathbb{T}). \quad (2.15)$$

Since we assume the parameterization is regular; the weighted  $L^2$ -inner product and the  $L^2$  space are equivalent to the usual one, which is independent of  $t$ . The Sobolev space  $H^1(\mathbb{T})$  is defined as

$$H^1(\mathbb{T}) := \{u : \mathbb{T} \rightarrow \mathbb{R} \mid u \in L^2(\mathbb{T}), \partial_s u \in L^2(\mathbb{T})\}. \quad (2.16)$$

Moreover, we can extend the above definitions to the functions in  $[L^2(\mathbb{T})]^2$  and  $[H^1(\mathbb{T})]^2$ .

Multiplying a test function  $\phi \in H^1(\mathbb{T})$  to (2.13a), integrating over  $\Gamma(t)$  and taking integration by parts, we obtain

$$\left( \mathbf{n} \cdot \partial_t \mathbf{X}, \phi \right)_{\Gamma(t)} = - \left( \partial_s \mu, \partial_s \phi \right)_{\Gamma(t)}. \quad (2.17)$$

Similarly, by multiplying a test function  $\omega = (\omega_1, \omega_2)^T \in [H^1(\mathbb{T})]^2$  to (2.13b), we deduce that

$$\left( \mu \mathbf{n}, \omega \right)_{\Gamma(t)} = \left( \mathbf{G}_k(\mathbf{n}) \partial_s \mathbf{X}, \partial_s \omega \right)_{\Gamma(t)}. \quad (2.18)$$

Based on the two equations (2.17) and (2.18), the new variational formulation for the conservative form (2.13) can be stated as follows: Suppose the initial curve  $\Gamma_0 := \mathbf{X}(\cdot, 0) = (x(\cdot, 0), y(\cdot, 0))^T \in [H^1(\mathbb{T})]^2$  and the initial weighted curvature  $\mu(\cdot, 0) := \mu_0(\cdot) \in H^1(\mathbb{T})$ , then for any  $t > 0$ , find the solution  $(\mathbf{X}(\cdot, t), \mu(\cdot, t)) \in [H^1(\mathbb{T})]^2 \times H^1(\mathbb{T})$  satisfying

$$\left( \mathbf{n} \cdot \partial_t \mathbf{X}, \varphi \right)_{\Gamma(t)} + \left( \partial_s \mu, \partial_s \varphi \right)_{\Gamma(t)} = 0, \quad \forall \varphi \in H^1(\mathbb{T}), \quad (2.19a)$$

$$\left( \mu \mathbf{n}, \omega \right)_{\Gamma(t)} - \left( \mathbf{G}_k(\mathbf{n}) \partial_s \mathbf{X}, \partial_s \omega \right)_{\Gamma(t)} = 0, \quad \forall \omega \in [H^1(\mathbb{T})]^2. \quad (2.19b)$$

Denote the area of the region enclosed by  $\Gamma(t)$  as  $A(t)$  and the free interfacial energy of  $\Gamma(t)$  as  $W(t)$ , which are given by

$$A(t) := \int_{\Gamma(t)} y(\rho, t) \partial_\rho x(\rho, t) d\rho, \quad W(t) := \int_{\Gamma(t)} \gamma(\mathbf{n}) ds, \quad t \geq 0. \quad (2.20)$$

We can show that the two geometric properties, i.e. area conservation and energy dissipation, still hold for the weak formulation (2.19).

**Proposition 2.1 (area conservation and energy dissipation)** *Suppose  $\Gamma(t)$  is given by the solution  $(X(\cdot, t), \mu(\cdot, t))$  of the variational formulation (2.19), we have*

$$A(t) \equiv A(0), \quad W(t) \leq W(t_1) \leq W(0), \quad \forall t \geq t_1 \geq 0. \quad (2.21)$$

The proof is similar to [32, Proposition 2.1] and details are omitted for brevity.

## 2.4 A semi-discretization in space

To obtain the spatial discretization, suppose  $N > 2$  be an integer,  $h = \frac{1}{N}$  is the mesh size,  $\mathbb{T} = [0, 1] = \cup_{j=1}^N I_j := \cup_{j=1}^N [\rho_{j-1}, \rho_j]$  with  $\rho_j = jh, j = 0, 1, \dots, N$ , and we know  $\rho_N = \rho_0$  by periodic. The closed curve  $\Gamma(t) = X(\cdot, t)$  is approximated by the closed line segments  $\Gamma^h(t) = X^h(\cdot, t) = (x^h(\cdot, t), y^h(\cdot, t))^T$  satisfying  $X^h(\rho_j, 0) = X(\rho_j, 0)$ . And the discretization for test function space  $H^1(\mathbb{T})$  with respect to  $\Gamma^h(t)$  is given by the following space of piecewise linear finite element functions

$$\mathbb{K}^h = \mathbb{K}^h(\mathbb{T}) := \{u \in C(\mathbb{T}) \mid u|_{I_j} \in \mathcal{P}^1(I_j), \forall 1 \leq j \leq N\}, \quad (2.22)$$

where  $\mathcal{P}^1(I_j)$  is the set of polynomials defined on  $I_j$  of degree  $\leq 1$ . The mass lumped inner product for two function  $u, v \in \mathbb{K}^h(\mathbb{T})$  with respect to  $\Gamma^h(t)$  is defined as

$$(u, v)_{\Gamma^h(t)}^h := \frac{1}{2} \sum_{j=1}^N |\mathbf{h}_j(t)| \left( (u \cdot v)(\rho_{j-1}^+) + (u \cdot v)(\rho_j^-) \right). \quad (2.23)$$

where  $\mathbf{h}_j(t) = X^h(\rho_j, t) - X^h(\rho_{j-1}, t)$ , and  $u(\rho_j^\pm) = \lim_{\rho \rightarrow \rho_j^\pm} u(\rho)$ . We note this mass

lumped inner product is also valid for  $[\mathbb{K}^h]^2$  and the piecewise constant vector-valued functions with possible jump discontinuities at  $\rho_j$  for  $0 \leq j \leq N$ .

The discretized unit normal vector  $\mathbf{n}^h(t)$ , unit tangential vector  $\boldsymbol{\tau}^h(t)$ , and the  $\boldsymbol{\xi}$ -vector  $\boldsymbol{\xi}^h(t)$  are such piecewise constant vectors on  $\Gamma^h(t)$ , which are given as

$$\mathbf{n}_j^h := \mathbf{n}^h|_{I_j} = -\frac{\mathbf{h}_j^\perp}{|\mathbf{h}_j|}, \quad \boldsymbol{\tau}_j^h := \boldsymbol{\tau}^h|_{I_j} = (\mathbf{n}_j^h)^\perp, \quad \boldsymbol{\xi}_j^h := \boldsymbol{\xi}^h|_{I_j} = \nabla \gamma(\mathbf{p})|_{\mathbf{p}=\mathbf{n}_j^h}. \quad (2.24)$$

Here we use  $\mathbf{n}^h$  to represent  $\mathbf{n}^h(t)$  for short. To make sure  $\mathbf{n}^h, \boldsymbol{\tau}^h, \boldsymbol{\xi}^h$  are well defined, we need the following assumption on  $\mathbf{h}_j(t)$

$$\min_{1 \leq j \leq N} |\mathbf{h}_j(t)| > 0, \quad \forall t \geq 0. \quad (2.25)$$

After giving all the continuous objects their discretized versions, we can state the spatial semi-discretization as follows: Let  $\Gamma_0^h := \mathbf{X}^h(\cdot, 0) \in [\mathbb{K}^h]^2$ ,  $\mu^h(\cdot, 0) \in \mathbb{K}^h$  be the approximations of  $\Gamma_0 := \mathbf{X}_0(\cdot)$ ,  $\mu_0(\cdot)$ , respectively, with  $\mathbf{X}^h(\rho_j, 0) = \mathbf{X}(\rho_j, 0)$ ,  $\mu^h(\rho_j, 0) = \mu_0(\rho_j)$  for  $0 \leq j \leq N$ , find the solution  $(\mathbf{X}^h(\cdot, t), \mu^h(\cdot, t)) \in [\mathbb{K}^h]^2 \times \mathbb{K}^h$ , such that

$$\left( \mathbf{n}^h \cdot \partial_t \mathbf{X}^h, \varphi^h \right)_{\Gamma^h(t)}^h + \left( \partial_s \mu^h, \partial_s \varphi^h \right)_{\Gamma^h(t)}^h = 0, \quad \forall \varphi^h \in \mathbb{K}^h, \quad (2.26a)$$

$$\left( \mu^h \mathbf{n}^h, \omega^h \right)_{\Gamma^h(t)}^h - \left( \mathbf{G}_k(\mathbf{n}^h) \partial_s \mathbf{X}^h, \partial_s \omega^h \right)_{\Gamma^h(t)}^h = 0, \quad \forall \omega^h \in [\mathbb{K}^h]^2, \quad (2.26b)$$

where

$$\mathbf{G}_k(\mathbf{n}^h)|_{I_j} = \gamma(\mathbf{n}_j^h) I_2 - \mathbf{n}_j^h (\boldsymbol{\xi}_j^h)^T + \boldsymbol{\xi}_j^h (\mathbf{n}_j^h)^T + k(\mathbf{n}_j^h) \mathbf{n}_j^h (\mathbf{n}_j^h)^T, \quad (2.27)$$

and the discretized derivative  $\partial_s$  for a scalar and vector valued functions  $f$  and  $\mathbf{f}$ , respectively, are given as

$$\partial_s f|_{I_j} := \frac{f(\rho_j) - f(\rho_{j-1})}{|\mathbf{h}_j|}, \quad \partial_s \mathbf{f}|_{I_j} := \frac{\mathbf{f}(\rho_j) - \mathbf{f}(\rho_{j-1})}{|\mathbf{h}_j|}, \quad (2.28)$$

and assumption (2.25) ensures  $\partial_s f$  and  $\partial_s \mathbf{f}$  are piecewise constant functions with possible jump discontinuities at  $\rho_j$  for  $0 \leq j \leq N$ , thus the mass lumped inner product terms like  $\left( \partial_s \mu^h, \partial_s \varphi^h \right)_{\Gamma^h(t)}^h$  in (2.26) are well defined.

Denote the enclosed area and the total energy of the closed line segments  $\Gamma^h(t)$  as  $A^h(t)$  and  $W^h(t)$ , respectively, which are given by

$$A^h(t) = \frac{1}{2} \sum_{j=1}^N (x_j^h(t) - x_{j-1}^h(t))(y_j^h(t) + y_{j-1}^h(t)), \quad W^h(t) = \sum_{j=1}^N |\mathbf{h}_j(t)| \gamma(\mathbf{n}_j^h), \quad (2.29)$$

where  $x_j^h(t) := x^h(\rho_j, t)$ ,  $y_j^h(t) := y^h(\rho_j, t)$ ,  $\forall 0 \leq j \leq N$ . Then following the same statement in the proof of [32, Proposition 3.1], we know that the spatial discretization (2.26) still preserves the two geometric properties.

**Proposition 2.2 (area conservation and energy dissipation)** *Suppose  $\Gamma^h(t)$  is given by the solution  $(\mathbf{X}^h(\cdot, t), \mu^h(\cdot, t))$  of (2.26), then we have*

$$A^h(t) \equiv A^h(0), \quad W^h(t) \leq W^h(t_1) \leq W^h(0), \quad \forall t \geq t_1 \geq 0. \quad (2.30)$$

## 2.5 A structure-preserving PFEM

We then consider the full discretization. Let  $\tau$  be the uniform time step, and  $\Gamma^m = \mathbf{X}^m(\cdot) \in [\mathbb{K}^h]^2$  be the approximation of  $\Gamma^h(t_m) = \mathbf{X}^h(\cdot, t_m)$ ,  $\forall m \geq 0$ , where  $t_m := m\tau$ . Suppose  $\mathbf{h}^m := \mathbf{X}^m(\rho_j) - \mathbf{X}^m(\rho_{j-1})$ , we can similarly give the definitions for the mass lumped inner product  $(\cdot, \cdot)_{\Gamma^m}^h$  as well as the unit normal vector  $\mathbf{n}^m$ , the unit tangential vector  $\boldsymbol{\tau}^m$ , and the  $\boldsymbol{\xi}$ -vector  $\boldsymbol{\xi}^m$  with respect to  $\Gamma^m$ . By adopting



the backward Euler method, the fully-implicit structure-preserving discretization of PFEM for anisotropic surface diffusion (2.7) can then be given as:

Suppose the initial approximation  $\Gamma^0(\cdot) \in [\mathbb{K}^h]^2$  is given by  $\mathbf{X}^0(\rho_j) = \mathbf{X}_0(\rho_j), \forall 0 \leq j \leq N$ . For any  $m = 0, 1, 2, \dots$ , find the solution  $(\mathbf{X}^m(\cdot) = (x^m(\cdot), y^m(\cdot))^T, \mu^m(\cdot)) \in [\mathbb{K}^h]^2 \times \mathbb{K}^h$ , such that

$$\left( \mathbf{n}^{m+\frac{1}{2}} \cdot \frac{\mathbf{X}^{m+1} - \mathbf{X}^m}{\tau}, \varphi^h \right)_{\Gamma^m}^h + \left( \partial_s \mu^{m+1}, \partial_s \varphi^h \right)_{\Gamma^m}^h = 0, \quad \forall \varphi^h \in \mathbb{K}^h, \quad (2.31a)$$

$$\left( \mu^{m+1} \mathbf{n}^{m+\frac{1}{2}}, \omega^h \right)_{\Gamma^m}^h - \left( \mathbf{G}_k(\mathbf{n}^m) \partial_s \mathbf{X}^{m+1}, \partial_s \omega^h \right)_{\Gamma^m}^h = 0, \quad \forall \omega^h \in [\mathbb{K}^h]^2, \quad (2.31b)$$

where

$$\mathbf{G}_k(\mathbf{n}^m)|_{I_j} = \gamma(\mathbf{n}_j^m) I_2 - \mathbf{n}_j^m (\boldsymbol{\xi}_j^m)^T + \boldsymbol{\xi}_j^m (\mathbf{n}_j^m)^T + k(\mathbf{n}_j^m) \mathbf{n}_j^m (\mathbf{n}_j^m)^T, \quad (2.32)$$

and

$$\mathbf{n}^{m+\frac{1}{2}} := -\frac{1}{2} \frac{1}{|\partial_\rho \mathbf{X}^m|} (\partial_\rho \mathbf{X}^m + \partial_\rho \mathbf{X}^{m+1})^\perp. \quad (2.33)$$

The SP-PFEM (2.31) is fully-implicit, and we can apply Newton's iterative method proposed in [7] to solve it numerically. If  $\mathbf{n}^{m+\frac{1}{2}}$  is replaced by  $\mathbf{n}^m$ , then (2.31) becomes semi-implicit. However, the clever choice  $\mathbf{n}^{m+\frac{1}{2}}$  is critical in preserving the area conservation, and the semi-implicit PFEM can only preserve the energy dissipation property.

## 2.6 Main results

Denote the enclosed area and the total energy of the closed line segments  $\Gamma^m$  as  $A^m$  and  $W^m$ , respectively, which are given by

$$A^m = \frac{1}{2} \sum_{j=1}^N (x^m(\rho_j) - x^m(\rho_{j-1}))(y^m(\rho_j) + y^m(\rho_{j-1})), \quad (2.34a)$$

$$W^m = \sum_{j=1}^N |\mathbf{h}_j^m| \gamma(\mathbf{n}_j^m). \quad (2.34b)$$

Introduce two auxiliary functions  $P_\alpha(\mathbf{n}, \hat{\mathbf{n}}), Q(\mathbf{n}, \hat{\mathbf{n}})$  as

$$P_\alpha(\mathbf{n}, \hat{\mathbf{n}}) := 2\sqrt{(\gamma(\mathbf{n}) + \alpha(\hat{\mathbf{n}} \cdot \mathbf{n}^\perp)^2)\gamma(\mathbf{n})}, \quad \forall \mathbf{n} \in \mathbb{S}^1, \quad \alpha \geq 0, \quad (2.35a)$$

$$Q(\mathbf{n}, \hat{\mathbf{n}}) := \gamma(\hat{\mathbf{n}}) + \gamma(\mathbf{n})(\mathbf{n} \cdot \hat{\mathbf{n}}) - (\boldsymbol{\xi} \cdot \mathbf{n}^\perp)(\hat{\mathbf{n}} \cdot \mathbf{n}^\perp), \quad \forall \mathbf{n}, \hat{\mathbf{n}} \in \mathbb{S}^1, \quad (2.35b)$$

we define the minimal stabilizing function  $k_0(\mathbf{n})$  as (its existence will be given in next section)

$$k_0(\mathbf{n}) := \inf\{\alpha \geq 0 : P_\alpha(\mathbf{n}, \hat{\mathbf{n}}) - Q(\mathbf{n}, \hat{\mathbf{n}}) \geq 0, \forall \hat{\mathbf{n}} \in \mathbb{S}^1\}, \quad \forall \mathbf{n} \in \mathbb{S}^1. \quad (2.36)$$

For the SP-PFEM (2.31), we have

**Theorem 2.1 (structure-preserving)** Suppose  $\gamma(\mathbf{n})$  satisfies

$$3\gamma(\mathbf{n}) > \gamma(-\mathbf{n}), \quad \forall \mathbf{n} \in \mathbb{S}^1, \quad \gamma(\mathbf{p}) \in C^2(\mathbb{R}^2 \setminus \{\mathbf{0}\}), \quad (2.37)$$

and take the stabilizing function  $k(\mathbf{n}) \geq k_0(\mathbf{n})$  for  $\mathbf{n} \in \mathbb{S}^1$ , then the SP-PFEM (2.31) preserves the two geometric properties in the discrete level, i.e.,

$$A^{m+1} \equiv A^0, \quad W^{m+1} \leq W^m \leq \dots \leq W^0, \quad \forall m \geq 0. \quad (2.38)$$

The area conservation part is a direct result of [7, Theorem 2.1]. And the energy dissipation will be proved in the next section.

### 3 Energy dissipation of the SP-PFEM (2.31)

In this section, we first show if  $\gamma(\mathbf{n})$  satisfies (2.37), the minimal stabilizing function  $k_0(\mathbf{n})$  defined in (2.36) is well-defined, thus we can always choose a nonnegative stabilizing function  $k(\mathbf{n}) \geq k_0(\mathbf{n})$  for  $\mathbf{n} \in \mathbb{S}^1$ . After that, we will use  $k_0(\mathbf{n})$  to give the proof of the unconditional energy stability part of the main theorem 2.1.

#### 3.1 Existence of the minimal stabilizing function $k_0(\mathbf{n})$ defined in (2.36)

From the definition of  $k_0(\mathbf{n})$  in (2.36), we observe that if  $(\hat{\mathbf{n}} \cdot \mathbf{n}^\perp)^2 > 0$ , then intuitively for sufficiently large  $\alpha$ , we know the  $P_\alpha(\mathbf{n}, \hat{\mathbf{n}}) \geq Q(\mathbf{n}, \hat{\mathbf{n}})$ . But this approach will fail when  $(\hat{\mathbf{n}} \cdot \mathbf{n}^\perp)^2 = 0$ , and this can happen if  $\hat{\mathbf{n}} = \pm \mathbf{n}$ , which suggests us to treat the two cases  $\hat{\mathbf{n}} \cdot \mathbf{n} \geq 0$  and  $\hat{\mathbf{n}} \cdot \mathbf{n} \leq 0$  separately. To simplify the notations, we introduce a compact set  $\mathbb{S}_\mathbf{n}^1$  as

$$\mathbb{S}_\mathbf{n}^1 := \{\hat{\mathbf{n}} \in \mathbb{S}^1 \mid \mathbf{n} \cdot \hat{\mathbf{n}} \geq 0\}, \quad \mathbf{n} \in \mathbb{S}^1. \quad (3.1)$$

Then  $\mathbf{n} \cdot \hat{\mathbf{n}} \geq 0 \iff \hat{\mathbf{n}} \in \mathbb{S}_\mathbf{n}^1$ , and  $\mathbf{n} \cdot \hat{\mathbf{n}} \leq 0 \iff \hat{\mathbf{n}} \in \mathbb{S}_{-\mathbf{n}}^1$ .

**Theorem 3.1** The  $k_0(\mathbf{n})$  defined as (2.36) is bounded if the condition (2.37) on  $\gamma(\mathbf{n})$  is satisfied.

*Proof* First we consider the case  $\hat{\mathbf{n}} \in \mathbb{S}_\mathbf{n}^1$ . Since  $\gamma(\mathbf{n})$  satisfies (2.37), we know  $\gamma(\mathbf{p}) \in C^2(\mathbb{R}^2 \setminus \{\mathbf{0}\})$ . Thus there exists a constant  $C_1 > 0$ , such that

$$\|\mathbf{H}_\gamma(\mathbf{p})\|_2 \leq C_1, \quad \forall \frac{1}{2} \leq |\mathbf{p}|^2 \leq 1, \quad (3.2)$$

here  $\mathbf{H}_\gamma$  is the Hessian matrix of  $\gamma(\mathbf{p})$ , and  $\|\cdot\|_2$  denotes the 2-norm.

By mean value theorem, we know for all  $\hat{\mathbf{n}} \in \mathbb{S}_\mathbf{n}^1$ , there exists a constant  $0 < c < 1$  such that

$$\gamma(\hat{\mathbf{n}}) = \gamma(\mathbf{n}) + \boldsymbol{\xi} \cdot (\hat{\mathbf{n}} - \mathbf{n}) + \frac{1}{2} (\hat{\mathbf{n}} - \mathbf{n})^T \mathbf{H}_\gamma(c\mathbf{n} + (1-c)\hat{\mathbf{n}}) (\hat{\mathbf{n}} - \mathbf{n}). \quad (3.3)$$

It is easy to see that  $|c\mathbf{n} + (1-c)\hat{\mathbf{n}}| \leq 1$  and  $|c\mathbf{n} + (1-c)\hat{\mathbf{n}}|^2 \geq c^2 + (1-c)^2 \geq \frac{1}{2}$ . Hence we know

$$\gamma(\hat{\mathbf{n}}) \leq \gamma(\mathbf{n}) + \boldsymbol{\xi} \cdot (\hat{\mathbf{n}} - \mathbf{n}) + \frac{C_1}{2} |\hat{\mathbf{n}} - \mathbf{n}|^2. \quad (3.4)$$

And notice that  $\xi \cdot \mathbf{n} = \gamma(\mathbf{n})$ , we can then get the following estimate of  $Q(\mathbf{n}, \hat{\mathbf{n}})$ :

$$\begin{aligned}
& Q(\mathbf{n}, \hat{\mathbf{n}}) - 2\gamma(\mathbf{n}) \\
& \leq \left( \gamma(\mathbf{n}) + \xi \cdot (\hat{\mathbf{n}} - \mathbf{n}) + \frac{C_1}{2} |\hat{\mathbf{n}} - \mathbf{n}|^2 \right) - \left( \xi \cdot \hat{\mathbf{n}} - (\xi \cdot \mathbf{n})(\hat{\mathbf{n}} \cdot \mathbf{n}) \right) \\
& \quad + \gamma(\mathbf{n})(\mathbf{n} \cdot \hat{\mathbf{n}}) - 2\gamma(\mathbf{n}) \\
& = 2\gamma(\mathbf{n})(\mathbf{n} \cdot \hat{\mathbf{n}} - 1) + \frac{C_1}{2} |\hat{\mathbf{n}} - \mathbf{n}|^2 \\
& = \left( \frac{C_1}{2} - \gamma(\mathbf{n}) \right) |\hat{\mathbf{n}} - \mathbf{n}|^2. \tag{3.5}
\end{aligned}$$

Here we use the fact  $\xi \cdot \hat{\mathbf{n}} = (\xi \cdot \mathbf{n})(\hat{\mathbf{n}} \cdot \mathbf{n}) + (\xi \cdot \mathbf{n}^\perp)(\hat{\mathbf{n}} \cdot \mathbf{n}^\perp)$  and  $|\hat{\mathbf{n}} - \mathbf{n}|^2 = 2 - 2\mathbf{n} \cdot \hat{\mathbf{n}}$ .

On the other hand, using the fact  $(\hat{\mathbf{n}} \cdot \mathbf{n}^\perp)^2 = 1 - (\hat{\mathbf{n}} \cdot \mathbf{n})^2 = \frac{|\hat{\mathbf{n}} - \mathbf{n}|^2}{2} (1 + \mathbf{n} \cdot \hat{\mathbf{n}})$ , we know that for  $\alpha > \gamma(\mathbf{n})$ , it holds

$$\begin{aligned}
P_\alpha(\mathbf{n}, \hat{\mathbf{n}}) - 2\gamma(\mathbf{n}) &= \frac{2\alpha(\hat{\mathbf{n}} \cdot \mathbf{n}^\perp)^2}{\sqrt{1 + \frac{\alpha}{\gamma(\mathbf{n})}(\hat{\mathbf{n}} \cdot \mathbf{n}^\perp)^2} + 1} \\
&\geq \frac{2\alpha(\hat{\mathbf{n}} \cdot \mathbf{n}^\perp)^2}{2\sqrt{1 + \frac{\alpha}{\gamma(\mathbf{n})}}} = \frac{\alpha(1 + \hat{\mathbf{n}} \cdot \mathbf{n})}{2\sqrt{1 + \frac{\alpha}{\gamma(\mathbf{n})}}} |\hat{\mathbf{n}} - \mathbf{n}|^2 \\
&\geq \frac{\sqrt{\gamma(\mathbf{n})(\alpha - \gamma(\mathbf{n}))}}{2} |\hat{\mathbf{n}} - \mathbf{n}|^2. \tag{3.6}
\end{aligned}$$

Combining (3.5) and (3.6), we know that for  $\alpha \geq \alpha_1 := \frac{(C_1 - 2\gamma(\mathbf{n}))^2 + \gamma^2(\mathbf{n})}{\gamma(\mathbf{n})} < \infty$ , it holds

$P_\alpha(\mathbf{n}, \hat{\mathbf{n}}) \geq Q(\mathbf{n}, \hat{\mathbf{n}}), \forall \hat{\mathbf{n}} \in \mathbb{S}_{\mathbf{n}}^1$ .

For the case  $\hat{\mathbf{n}} \in \mathbb{S}_{-\mathbf{n}}^1$ , by (2.37), when  $\hat{\mathbf{n}} = -\mathbf{n}$ , we know that

$$\begin{aligned}
Q(\mathbf{n}, -\mathbf{n}) &= \gamma(-\mathbf{n}) + \gamma(\mathbf{n})(\mathbf{n} \cdot (-\mathbf{n})) - (\xi \cdot \mathbf{n}^\perp)(-\mathbf{n} \cdot \mathbf{n}^\perp) \\
&< 3\gamma(\mathbf{n}) - \gamma(\mathbf{n}) = 2\gamma(\mathbf{n}). \tag{3.7}
\end{aligned}$$

Thus for  $\alpha = 0 := \alpha_{-\mathbf{n}} < \infty$ , we know  $P_0(\mathbf{n}, -\mathbf{n}) = 2\gamma(\mathbf{n}) > Q(\mathbf{n}, -\mathbf{n})$ . By continuity of  $P_\alpha$  and  $Q$ , there exists an open set  $\mathcal{O}_{-\mathbf{n},0} \subset \mathbb{S}^1$  such that  $-\mathbf{n} \in \mathcal{O}_{-\mathbf{n},0}$ , and for all  $\hat{\mathbf{n}} \in \mathcal{O}_{-\mathbf{n},0}$  and  $\alpha \geq 0$ , we have  $P_\alpha(\mathbf{n}, \hat{\mathbf{n}}) - Q(\mathbf{n}, \hat{\mathbf{n}}) \geq 0$ . For a given  $\mathbf{p} \in \mathbb{S}_{-\mathbf{n}}^1, \mathbf{p} \neq -\mathbf{n}$ , we know that  $(\mathbf{p} \cdot \mathbf{n}^\perp)^2 > 0$ . Therefore we can choose a sufficiently large but finite  $\alpha_{\mathbf{p}} < \infty$ , such that  $P_{\alpha_{\mathbf{p}}}(\mathbf{n}, \mathbf{p}) - Q(\mathbf{n}, \mathbf{p}) > 0$ . And by the same argument, there exists an open set  $\mathcal{O}_{\mathbf{p},\alpha_{\mathbf{p}}} \subset \mathbb{S}^1$ , such that  $\mathbf{p} \in \mathcal{O}_{\mathbf{p},\alpha_{\mathbf{p}}}$  and  $P_\alpha(\mathbf{n}, \hat{\mathbf{n}}) - Q(\mathbf{n}, \hat{\mathbf{n}}) \geq 0, \forall \hat{\mathbf{n}} \in \mathcal{O}_{\mathbf{p},\alpha_{\mathbf{p}}}, \alpha \geq \alpha_{\mathbf{p}}$ . And we obtain an open cover for  $\mathbb{S}_{-\mathbf{n}}^1$  as

$$\mathbb{S}_{-\mathbf{n}}^1 \subset \bigcup_{\mathbf{p} \in \mathbb{S}_{-\mathbf{n}}^1} \mathcal{O}_{\mathbf{p},\alpha_{\mathbf{p}}}. \tag{3.8}$$

Since  $\mathbb{S}_{-\mathbf{n}}^1$  is compact, by open cover theorem, there is a finite set of vectors  $\mathbf{p}_1, \dots, \mathbf{p}_M \in \mathbb{S}_{-\mathbf{n}}^1$ , such that

$$\mathbb{S}_{-\mathbf{n}}^1 \subset \bigcup_{i=1}^M \mathcal{O}_{\mathbf{p}_i,\alpha_{\mathbf{p}_i}}. \tag{3.9}$$

If we take  $\alpha_2 := \max_{1 \leq i \leq M} \alpha_{\mathbf{p}_i} < \infty$ , we have  $P_\alpha(\mathbf{n}, \hat{\mathbf{n}}) - Q(\mathbf{n}, \hat{\mathbf{n}}) \geq 0, \forall \hat{\mathbf{n}} \in \mathbb{S}_{-\mathbf{n}}^1, \alpha \geq \alpha_2$ , hence

$$\infty > \max(\alpha_1, \alpha_2) \in \{\alpha \geq 0 : P_\alpha(\mathbf{n}, \hat{\mathbf{n}}) - Q(\mathbf{n}, \hat{\mathbf{n}}) \geq 0, \forall \hat{\mathbf{n}} \in \mathbb{S}^1\}. \quad (3.10)$$

Which means  $k_0(\mathbf{n}) = \inf \{\alpha \geq 0 : P_\alpha(\mathbf{n}, \hat{\mathbf{n}}) - Q(\mathbf{n}, \hat{\mathbf{n}}) \geq 0, \forall \hat{\mathbf{n}} \in \mathbb{S}^1\} < \infty$ .  $\square$

*Remark 3.1* The  $\hat{\mathbf{n}} \in \mathbb{S}_{\mathbf{n}}^1$  part only requires inequality (3.4), thus condition  $\gamma(\mathbf{p}) \in C^2(\mathbb{R}^2 \setminus \{\mathbf{0}\})$  can be relaxed to  $\gamma(\mathbf{p})$  is piecewise  $C^2(\mathbb{R}^2 \setminus \{\mathbf{0}\})$ . And the condition  $3\gamma(\mathbf{n}) > \gamma(-\mathbf{n})$  is to ensure the existence of  $\mathcal{O}_{-\mathbf{n}, 0}$ , which suggests we may find a larger  $\alpha_{-\mathbf{n}} > 0$  such that  $\mathcal{O}_{-\mathbf{n}, \alpha_{-\mathbf{n}}}$  exists for  $\gamma(\mathbf{n})$  satisfies  $3\gamma(\mathbf{n}) \geq \gamma(-\mathbf{n})$ . And by the same argument, we can show such  $\mathcal{O}_{-\mathbf{n}, \alpha_{-\mathbf{n}}}$  exists if and only if  $\xi(\mathbf{n}_i) = \gamma(\mathbf{n}_i)\mathbf{n}_i \iff 3\gamma(\mathbf{n}_i) = \gamma(-\mathbf{n}_i)$ .

By the existence of  $k_0(\mathbf{n})$ , once the  $\gamma(\mathbf{n})$  is given, the minimal stabilizing function  $k_0(\mathbf{n})$  is then determined, i.e. there is a map from  $\gamma(\mathbf{n})$  to  $k_0(\mathbf{n})$ . Similar to the proof when  $\gamma(\mathbf{n})$  is symmetric, i.e.  $\gamma(\mathbf{n}) = \gamma(-\mathbf{n})$  in [2, 7], we can show such map is a sub-linear with respect to  $\gamma(\mathbf{n})$  when it satisfies (2.37).

**Lemma 3.1 (positive homogeneity and subadditivity)** *Let  $\gamma_1(\mathbf{n}), \gamma_2(\mathbf{n})$  and  $\gamma_3(\mathbf{n})$  be three functions satisfying (2.37) with minimal stabilizing functions  $k_1(\mathbf{n}), k_2(\mathbf{n})$  and  $k_3(\mathbf{n})$ , respectively, then we have*

- (i) if  $\gamma_2(\mathbf{n}) = c\gamma_1(\mathbf{n})$ , where  $c > 0$  is a positive number, then  $k_2(\mathbf{n}) = ck_1(\mathbf{n})$ ; and
- (ii) if  $\gamma_3(\mathbf{n}) = \gamma_1(\mathbf{n}) + \gamma_2(\mathbf{n})$ , then  $k_3(\mathbf{n}) \leq k_1(\mathbf{n}) + k_2(\mathbf{n})$ .

The proof is similar to [3, Lemma 4.4], and is omitted for brevity.

### 3.2 Proof of the energy dissipation in (2.38)

To prove the main result, we first need the following lemma:

**Lemma 3.2** *Suppose  $\mathbf{h}, \hat{\mathbf{h}}$  are two non-zero vectors in  $\mathbb{R}^2$  and  $\mathbf{n} = -\frac{\mathbf{h}^\perp}{|\mathbf{h}|}, \hat{\mathbf{n}} = -\frac{\hat{\mathbf{h}}^\perp}{|\hat{\mathbf{h}}|}$  to be the corresponding unit normal vectors. Then for any  $k(\mathbf{n}) \geq k_0(\mathbf{n})$ , the following inequality holds*

$$\frac{1}{|\mathbf{h}|} \left( \mathbf{G}_k(\mathbf{n})\hat{\mathbf{h}} \right) \cdot (\hat{\mathbf{h}} - \mathbf{h}) \geq |\hat{\mathbf{h}}|\gamma(\hat{\mathbf{n}}) - |\mathbf{h}|\gamma(\mathbf{n}). \quad (3.11)$$

*Proof* By applying the definition of  $\mathbf{G}_k(\mathbf{n})$  in (2.8) and  $P_\alpha(\mathbf{n}, \hat{\mathbf{n}})$  in (2.35a), and noticing  $\hat{\mathbf{h}} = \hat{\mathbf{n}}^\perp |\hat{\mathbf{h}}|$ ,  $\mathbf{n} \cdot \hat{\mathbf{n}}^\perp = -\hat{\mathbf{n}} \cdot \mathbf{n}^\perp$ , the term  $\frac{1}{|\hat{\mathbf{h}}|} (\mathbf{G}_k(\mathbf{n}) \hat{\mathbf{h}}) \cdot \hat{\mathbf{h}}$  can be simplified as

$$\begin{aligned}
& \frac{1}{|\hat{\mathbf{h}}|} (\mathbf{G}_k(\mathbf{n}) \hat{\mathbf{h}}) \cdot \hat{\mathbf{h}} \\
&= \frac{1}{|\hat{\mathbf{h}}|} \left[ \left( (\gamma(\mathbf{n}) I_2 + k(\mathbf{n}) \mathbf{n}(\mathbf{n})^T) + (\boldsymbol{\xi}(\mathbf{n})^T - \mathbf{n}(\boldsymbol{\xi})^T) \right) \hat{\mathbf{h}} \right] \cdot \hat{\mathbf{h}} \\
&= \frac{1}{|\hat{\mathbf{h}}|} \left[ \left( \gamma(\mathbf{n}) I_2 + k(\mathbf{n}) \mathbf{n}(\mathbf{n})^T \right) \hat{\mathbf{h}} \right] \cdot \hat{\mathbf{h}} \\
&= \frac{1}{|\hat{\mathbf{h}}|} \left( \gamma(\mathbf{n}) |\hat{\mathbf{h}}|^2 + k(\mathbf{n}) (\mathbf{n} \cdot \hat{\mathbf{h}})^2 \right) \\
&= \frac{1}{|\hat{\mathbf{h}}|} \left( \gamma(\mathbf{n}) |\hat{\mathbf{h}}|^2 + k(\mathbf{n}) (\hat{\mathbf{n}} \cdot (\mathbf{n}^\perp)^2 |\hat{\mathbf{h}}|^2) \right) = \frac{|\hat{\mathbf{h}}|^2}{4|\hat{\mathbf{h}}|\gamma(\mathbf{n})} P_{k(\mathbf{n})}^2(\mathbf{n}, \hat{\mathbf{n}}). \quad (3.12)
\end{aligned}$$

Similarly, by applying the definition of  $\mathbf{G}_k(\mathbf{n})$  in (2.8) and  $\mathcal{Q}(\mathbf{n}, \hat{\mathbf{n}})$  in (2.35b), and noticing  $\mathbf{h} = \mathbf{n}^\perp |\mathbf{h}|$ ,  $\hat{\mathbf{h}} = \hat{\mathbf{n}}^\perp |\hat{\mathbf{h}}|$ ,  $\mathbf{h} \cdot \hat{\mathbf{h}} = \mathbf{n} \cdot \hat{\mathbf{n}} |\mathbf{h}| |\hat{\mathbf{h}}|$ ,  $\mathbf{n} \cdot \hat{\mathbf{n}}^\perp = -\hat{\mathbf{n}} \cdot \mathbf{n}^\perp$ , the term  $\frac{1}{|\hat{\mathbf{h}}|} (\mathbf{G}_k(\mathbf{n}) \hat{\mathbf{h}}) \cdot \mathbf{h}$  can be simplified as

$$\begin{aligned}
& \frac{1}{|\hat{\mathbf{h}}|} (\mathbf{G}_k(\mathbf{n}) \hat{\mathbf{h}}) \cdot \mathbf{h} = \frac{1}{|\hat{\mathbf{h}}|} (\mathbf{G}_k^T(\mathbf{n}) \mathbf{h}) \cdot \hat{\mathbf{h}} \\
&= \frac{1}{|\hat{\mathbf{h}}|} \left[ \left( (\gamma(\mathbf{n}) I_2 + \mathbf{n}(\boldsymbol{\xi})^T) + (-\boldsymbol{\xi}(\mathbf{n})^T + k(\mathbf{n}) \mathbf{n}(\mathbf{n})^T) \right) \mathbf{h} \right] \cdot \hat{\mathbf{h}} \\
&= \frac{1}{|\hat{\mathbf{h}}|} \left[ \left( \gamma(\mathbf{n}) I_2 + \mathbf{n}(\boldsymbol{\xi})^T \right) \mathbf{h} \right] \cdot \hat{\mathbf{h}} \\
&= \frac{1}{|\hat{\mathbf{h}}|} [\gamma(\mathbf{n}) (\mathbf{h} \cdot \hat{\mathbf{h}}) + (\boldsymbol{\xi} \cdot \mathbf{h}) (\mathbf{n} \cdot \hat{\mathbf{h}})] \\
&= |\hat{\mathbf{h}}| (\gamma(\mathbf{n}) (\mathbf{n} \cdot \hat{\mathbf{n}}) + (\boldsymbol{\xi} \cdot \mathbf{n}^\perp) (\mathbf{n} \cdot \hat{\mathbf{n}}^\perp)) \\
&= |\hat{\mathbf{h}}| (\gamma(\mathbf{n}) (\mathbf{n} \cdot \hat{\mathbf{n}}) - (\boldsymbol{\xi} \cdot \mathbf{n}^\perp) (\hat{\mathbf{n}} \cdot \mathbf{n}^\perp)) = |\hat{\mathbf{h}}| (\mathcal{Q}(\mathbf{n}, \hat{\mathbf{n}}) - \gamma(\hat{\mathbf{n}})). \quad (3.13)
\end{aligned}$$

Finally, combining the definition of  $k_0(\mathbf{n})$  (2.36), (3.12), (3.13), and the fact  $\frac{a^2}{4|b|\gamma(\mathbf{n})} \geq -ab + |b|\gamma(\mathbf{n})b^2$  yields that

$$\begin{aligned}
\frac{1}{|\hat{\mathbf{h}}|} (\mathbf{G}_k(\mathbf{n}) \hat{\mathbf{h}}) \cdot (\hat{\mathbf{h}} - \mathbf{h}) &= \frac{|\hat{\mathbf{h}}|^2}{4|\hat{\mathbf{h}}|\gamma(\mathbf{n})} P_{k(\mathbf{n})}^2(\mathbf{n}, \hat{\mathbf{n}}) - |\hat{\mathbf{h}}| (\mathcal{Q}(\mathbf{n}, \hat{\mathbf{n}}) - \gamma(\hat{\mathbf{n}})) \\
&\geq -|\hat{\mathbf{h}}| P_{k(\mathbf{n})} + |\hat{\mathbf{h}}|\gamma(\mathbf{n}) - |\hat{\mathbf{h}}| (P_{k(\mathbf{n})}(\mathbf{n}, \hat{\mathbf{n}}) - \gamma(\hat{\mathbf{n}})) \\
&= |\hat{\mathbf{h}}|\gamma(\hat{\mathbf{n}}) - |\hat{\mathbf{h}}|\gamma(\mathbf{n}), \quad (3.14)
\end{aligned}$$

which validates (3.11).  $\square$

Now we can prove the energy dissipation part in our main result Theorem 2.1.

*Proof* The key point of the proof is to establish the following energy estimation

$$\left( \mathbf{G}_k(\mathbf{n}^m) \partial_s \mathbf{X}^{m+1}, \partial_s (\mathbf{X}^{m+1} - \mathbf{X}^m) \right)_{\Gamma^m}^h \geq W^{m+1} - W^m, \quad m \geq 0. \quad (3.15)$$

For any  $1 \leq j \leq N$ , take  $\mathbf{h} = \mathbf{h}_j^m$ ,  $\hat{\mathbf{h}} = \mathbf{h}_j^{m+1}$  in Lemma 3.2, we know that  $\mathbf{n} = -\frac{\mathbf{h}^\perp}{|\mathbf{h}|} = \mathbf{n}_j^m$ ,  $\hat{\mathbf{n}} = \mathbf{n}_j^{m+1}$ , and the following inequality holds

$$\frac{1}{|\mathbf{h}_j^m|} \left( \mathbf{G}_k(\mathbf{n}_j^m) \mathbf{h}_j^{m+1} \right) \cdot (\mathbf{h}_j^{m+1} - \mathbf{h}_j^m) \geq |\mathbf{h}_j^{m+1}| \gamma(\mathbf{n}_j^{m+1}) - |\mathbf{h}_j^m| \gamma(\mathbf{n}_j^m). \quad (3.16)$$

Take summation over  $1 \leq j \leq N$  for (3.16) and notice (2.23) and (2.34b), we have

$$\begin{aligned} & \left( \mathbf{G}_k(\mathbf{n}^m) \partial_s \mathbf{X}^{m+1}, \partial_s (\mathbf{X}^{m+1} - \mathbf{X}^m) \right)_{\Gamma^m}^h \\ &= \sum_{j=1}^N \left[ |\mathbf{h}_j^m| \left( \mathbf{G}_k(\mathbf{n}_j^m) \frac{\mathbf{h}_j^{m+1}}{|\mathbf{h}_j^m|} \right) \cdot \frac{\mathbf{h}_j^{m+1} - \mathbf{h}_j^m}{|\mathbf{h}_j^m|} \right] \\ &= \sum_{j=1}^N \left[ \frac{1}{|\mathbf{h}_j^m|} \left( \mathbf{G}_k(\mathbf{n}_j^m) \mathbf{h}_j^{m+1} \right) \cdot (\mathbf{h}_j^{m+1} - \mathbf{h}_j^m) \right] \\ &\geq \sum_{j=1}^N \left[ |\mathbf{h}_j^{m+1}| \gamma(\mathbf{n}_j^{m+1}) - |\mathbf{h}_j^m| \gamma(\mathbf{n}_j^m) \right] \\ &= W^{m+1} - W^m, \quad \forall m = 0, 1, \dots \end{aligned}$$

which proves the energy estimation in (3.15).

Finally, take  $\varphi^h = \mu^{m+1}$  in (2.31a) and  $\omega^h = \mathbf{X}^{m+1} - \mathbf{X}^m$  in (2.31b), we have

$$\begin{aligned} 0 &\geq -\tau \left( \partial_s \mu^{m+1}, \partial_s \mu^{m+1} \right)_{\Gamma^m}^h \\ &= \left( \mathbf{n}^{m+\frac{1}{2}} \cdot (\mathbf{X}^{m+1} - \mathbf{X}^m), \mu^{m+1} \right)_{\Gamma^m}^h \\ &= \left( \mathbf{G}_k(\mathbf{n}^m) \partial_s \mathbf{X}^{m+1}, \partial_s (\mathbf{X}^{m+1} - \mathbf{X}^m) \right)_{\Gamma^m}^h \geq W^{m+1} - W^m, \end{aligned}$$

this is true for any  $m$ ; therefore, the energy  $W^m$  decreases monotonically, and the proof is completed.  $\square$

*Remark 3.2* The condition  $\gamma(\mathbf{p}) \in C^2(\mathbb{R}^2 \setminus \{\mathbf{0}\})$  in (2.37) is natural, but  $3\gamma(\mathbf{n}) > \gamma(-\mathbf{n})$  looks quite complicated and seems not very sharp. However, the proof shows the condition  $3\gamma(\mathbf{n}) > \gamma(-\mathbf{n})$  is indeed natural! To see this, inequality (3.11) in Lemma 3.2 is essential in showing the energy estimate (3.15). And if we take  $\hat{\mathbf{h}} = -\mathbf{h}$  in Lemma 3.2, then  $\hat{\mathbf{n}} = -\mathbf{n}$ , and the inequality (3.11) becomes

$$2\gamma(\mathbf{n}) |\mathbf{h}| \geq |\mathbf{h}| \gamma(-\mathbf{n}) - \gamma(\mathbf{n}) |\mathbf{h}|, \quad (3.17)$$

which means  $3\gamma(\mathbf{n}) \geq \gamma(-\mathbf{n})$ . Our sufficient energy stable condition (2.37) just replaces  $\geq$  with  $>$ , thus is natural and **almost necessary**.

#### 4 Extension to other anisotropic geometric flows

In fact, the energy stable condition on  $\gamma(\mathbf{n})$  in (2.37), the definition of  $\mathbf{G}_k(\mathbf{n})$  in (2.8), the alternative expression for  $\mu$  in (2.10), and the definition of  $k_0(\mathbf{n})$  in (2.36) are independent of the anisotropic surface diffusion flow. Thus these definitions and even the proof of energy stability can be directly extended to other anisotropic geometric flows.

##### 4.1 For anisotropic curvature flow

Similar to (2.13), for the anisotropic curvature flow in (1.3), we have a conservative geometric PDE as

$$\mathbf{n} \cdot \partial_t \mathbf{X} = -\mu, \quad (4.1a)$$

$$\mu \mathbf{n} = -\partial_s (\mathbf{G}_k(\mathbf{n}) \partial_s \mathbf{X}). \quad (4.1b)$$

Suppose the initial curve  $\mathbf{X}(\cdot, 0) = (x(\cdot, 0), y(\cdot, 0))^T := \Gamma_0 \in [H^1(\mathbb{T})]^2$  and the initial weighted curvature  $\mu(\cdot, 0) := \mu_0(\cdot) \in H^1(\mathbb{T})$ . Based on the conservative form (4.1), the variational formulation for anisotropic curvature flow is as follows: For any  $t > 0$ , find the solution  $(\mathbf{X}(\cdot, t), \mu(\cdot, t)) \in [H^1(\mathbb{T})]^2 \times H^1(\mathbb{T})$  satisfying

$$\left( \mathbf{n} \cdot \partial_t \mathbf{X}, \varphi \right)_{\Gamma(t)} + \left( \mu, \varphi \right)_{\Gamma(t)} = 0, \quad \forall \varphi \in H^1(\mathbb{T}), \quad (4.2a)$$

$$\left( \mu \mathbf{n}, \omega \right)_{\Gamma(t)} - \left( \mathbf{G}_k(\mathbf{n}) \partial_s \mathbf{X}, \partial_s \omega \right)_{\Gamma(t)} = 0, \quad \forall \omega \in [H^1(\mathbb{T})]^2. \quad (4.2b)$$

And the SP-PFEM for the anisotropic curvature flow (4.2) is as follows: Suppose the initial approximation  $\Gamma^0(\cdot) \in [\mathbb{K}^h]^2$  is given by  $\mathbf{X}^0(\rho_j) = \mathbf{X}_0(\rho_j), \forall 0 \leq j \leq N$ , then for any  $m = 0, 1, 2, \dots$ , find the solution  $(\mathbf{X}^m(\cdot), \mu^m(\cdot)) \in [\mathbb{K}^h]^2 \times \mathbb{K}^h$ , such that

$$\left( \mathbf{n}^{m+\frac{1}{2}} \cdot \frac{\mathbf{X}^{m+1} - \mathbf{X}^m}{\tau}, \varphi^h \right)_{\Gamma^m} + \left( \mu^{m+1}, \varphi^h \right)_{\Gamma^m} = 0, \quad \forall \varphi^h \in \mathbb{K}^h, \quad (4.3a)$$

$$\left( \mu^{m+1} \mathbf{n}^{m+\frac{1}{2}}, \omega^h \right)_{\Gamma^m} - \left( \mathbf{G}_k(\mathbf{n}^m) \partial_s \mathbf{X}^{m+1}, \partial_s \omega^h \right)_{\Gamma^m} = 0, \quad \forall \omega^h \in [\mathbb{K}^h]^2. \quad (4.3b)$$

For the SP-PFEM (4.3), we have

**Theorem 4.1 (structure-preserving)** *Suppose  $\gamma(\mathbf{n})$  satisfies (2.37) and take a stabilizing function  $k(\mathbf{n}) \geq k_0(\mathbf{n})$ , then the SP-PFEM (4.3) preserves area decay rate and energy dissipation, i.e.,*

$$\frac{A^{m+1} - A^m}{\tau} = - \left( \mu^{m+1}, 1 \right)_{\Gamma^m}^h, \quad W^{m+1} \leq W^m \leq \dots \leq W^0, \quad \forall m \geq 0. \quad (4.4)$$

*Proof* From [7, Theorem 2.1], we know that

$$A^{m+1} - A^m = \left( \mathbf{n}^{m+\frac{1}{2}} \cdot (\mathbf{X}^{m+1} - \mathbf{X}^m), 1 \right)_{\Gamma^m}^h. \quad (4.5)$$

Thus by taking  $\varphi^h \equiv 1 \in \mathbb{K}^h$  in (4.3a), we know that

$$\frac{A^{m+1} - A^m}{\tau} = \left( \mathbf{n}^{m+\frac{1}{2}} \cdot \frac{\mathbf{X}^{m+1} - \mathbf{X}^m}{\tau}, 1 \right)_{\Gamma^m}^h = -(\mu^{m+1}, 1)_{\Gamma^m}^h, \quad (4.6)$$

which is the desired decay rate in (4.4).

For energy dissipation, we have already known that (3.15) is true. Taking  $\varphi^h = \mu^{m+1}$  in (4.3a) and  $\omega^h = \mathbf{X}^{m+1} - \mathbf{X}^m$  in (4.3b), we know that

$$\begin{aligned} 0 &\geq -\tau \left( \mu^{m+1}, \mu^{m+1} \right)_{\Gamma^m}^h \\ &= \left( \mathbf{G}_k(\mathbf{n}^m) \partial_s \mathbf{X}^{m+1}, \partial_s (\mathbf{X}^{m+1} - \mathbf{X}^m) \right)_{\Gamma^m}^h \geq W^{m+1} - W^m. \end{aligned}$$

Hence we complete the proof.  $\square$

#### 4.2 For area-conserved anisotropic curvature flow

Similarly, for the area-conserved anisotropic curvature flow in (1.3), the conservative geometric PDE is given as

$$\mathbf{n} \cdot \partial_t \mathbf{X} = -\mu + \lambda(t), \quad (4.7a)$$

$$\mu \mathbf{n} = -\partial_s (\mathbf{G}_k(\mathbf{n}) \partial_s \mathbf{X}), \quad (4.7b)$$

where  $\lambda(t)$  is given as (1.4) by replacing  $\lambda$  and  $\Gamma$  by  $\lambda(t)$  and  $\Gamma(t)$ , respectively. And the variational formulation can be derived in a similar way.

In order to design a structure-preserving full discretization, we need to properly discretize  $\lambda(t)$ . Denote  $\lambda^{m+\frac{1}{2}}$  with respect to  $\Gamma^m$  as

$$\lambda^{m+\frac{1}{2}} := \frac{(\mu^{m+1}, 1)_{\Gamma^m}^h}{(1, 1)_{\Gamma^m}^h}. \quad (4.8)$$

By adopting this  $\lambda^{m+\frac{1}{2}}$ , the SP-PFEM for the area-conserved anisotropic curvature flow in (1.3) is as follows: Suppose the initial approximation  $\Gamma^0(\cdot) \in [\mathbb{K}^h]^2$  is given by  $\mathbf{X}^0(\rho_j) = \mathbf{X}_0(\rho_j)$ ,  $\forall 0 \leq j \leq N$ ; for any  $m = 0, 1, 2, \dots$ , find the solution  $(\mathbf{X}^m(\cdot), \mu^m(\cdot)) \in [\mathbb{K}^h]^2 \times \mathbb{K}^h$ , such that

$$\left( \mathbf{n}^m \cdot \frac{\mathbf{X}^{m+1} - \mathbf{X}^m}{\tau}, \varphi^h \right)_{\Gamma^m}^h + \left( \mu^{m+1} - \lambda^{m+\frac{1}{2}}, \varphi^h \right)_{\Gamma^m}^h = 0, \quad \forall \varphi^h \in \mathbb{K}^h, \quad (4.9a)$$

$$\left( \mu^{m+1} \mathbf{n}^m, \omega^h \right)_{\Gamma^m}^h - \left( \mathbf{G}_k(\mathbf{n}^m) \partial_s \mathbf{X}^{m+1}, \partial_s \omega^h \right)_{\Gamma^m}^h = 0, \quad \forall \omega^h \in [\mathbb{K}^h]^2. \quad (4.9b)$$

For the above SP-PFEM (4.9), we have

**Theorem 4.2 (structure-preserving)** *Suppose  $\gamma(\mathbf{n})$  satisfies (2.37) and take a finite stabilizing function  $k(\mathbf{n}) \geq k_0(\mathbf{n})$ , then the SP-PFEM (4.3) is structure-preserving, i.e.,*

$$A^{m+1} \equiv A^0, \quad W^{m+1} \leq W^m \leq \dots \leq W^0, \quad \forall m \geq 0. \quad (4.10)$$



*Proof* For the area conservation, taking  $\varphi^h \equiv 1$  in (4.9a) yields that

$$\begin{aligned} \left( \mathbf{n}^{m+\frac{1}{2}} \cdot (\mathbf{X}^{m+1} - \mathbf{X}^m), 1 \right)_{\Gamma^m}^h &= -\tau \left( \mu^{m+1} - \lambda^{m+\frac{1}{2}}, 1 \right)_{\Gamma^m}^h \\ &= -\tau \left( \mu^{m+1}, 1 \right)_{\Gamma^m}^h + \tau \lambda^{m+\frac{1}{2}} \left( 1, 1 \right)_{\Gamma^m}^h \\ &= -\tau \left( \mu^{m+1}, 1 \right)_{\Gamma^m}^h + \tau \frac{\left( \mu^{m+1}, 1 \right)_{\Gamma^m}^h}{\left( 1, 1 \right)_{\Gamma^m}^h} \left( 1, 1 \right)_{\Gamma^m}^h \\ &= 0, \quad m \geq 0. \end{aligned}$$

By noting (4.4), we deduce that  $A^{m+1} - A^m = 0$ , which shows area conservation (2.34a).

For energy dissipation, by Cauchy-Schwarz inequality, we have

$$\begin{aligned} \left( \lambda^{m+\frac{1}{2}}, \mu^{m+1} \right)_{\Gamma^m}^h &= \lambda^{m+\frac{1}{2}} \left( 1, \mu^{m+1} \right)_{\Gamma^m}^h \\ &= \frac{1}{\left( 1, 1 \right)_{\Gamma^m}^h} \left( \left( 1, \mu^{m+1} \right)_{\Gamma^m}^h \right)^2 \\ &\leq \frac{1}{\left( 1, 1 \right)_{\Gamma^m}^h} \left( 1, 1 \right)_{\Gamma^m}^h \left( \mu^{m+1}, \mu^{m+1} \right)_{\Gamma^m}^h \\ &= \left( \mu^{m+1}, \mu^{m+1} \right)_{\Gamma^m}^h, \quad m \geq 0. \end{aligned}$$

Taking  $\varphi^h = \mu^{m+1}$  in (4.9a) and  $\omega^h = \mathbf{X}^{m+1} - \mathbf{X}^m$  in (4.9b), and adopting the energy estimation (3.15) yields that

$$W^{m+1} - W^m \leq -\tau \left( \mu^{m+1} - \lambda^{m+\frac{1}{2}}, \mu^{m+1} \right)_{\Gamma^m}^h \leq 0, \quad m \geq 0, \quad (4.11)$$

which implies the energy dissipation in (4.10).  $\square$

## 5 Numerical results

In this section, we present numerical experiments to illustrate the high performance of the proposed SP-PFEMs. The implementations and performances of the three SP-PFEMs are very similar. Thus in section 5.1, we only show test results of the SP-PFEM (2.31) for the anisotropic surface diffusion. The morphological evolutions for three anisotropic geometric flows are shown in section 5.2.

To compute the minimal stabilizing function  $k_0(\mathbf{n})$ , we first solve the optimization problem (2.36) for 20 uniformly distributed points  $\mathbf{n}_j \in \mathbb{S}^1$ , and then do linear interpolation for the intermediate points. In Newton's iteration, the tolerance value  $\varepsilon$  is set as  $10^{-12}$ .

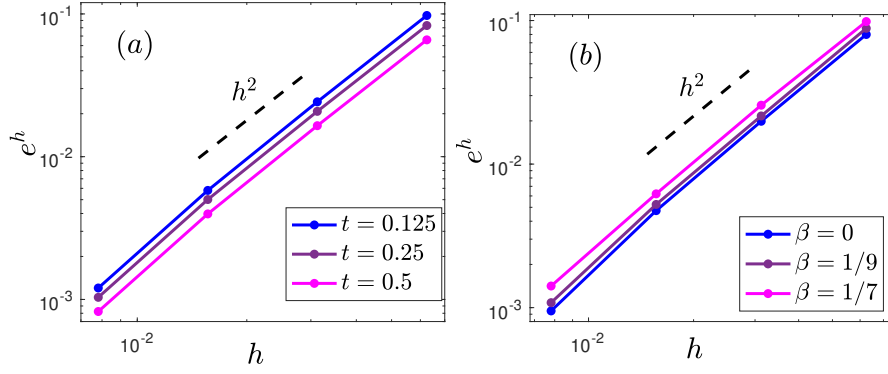


Fig. 5.1: Convergence rates of the SP-PFEM (2.31) with  $k(\mathbf{n}) = k_0(\mathbf{n})$  for: (a) anisotropy in Case I at different times  $t = 0.125, 0.25, 0.5$ ; and (b) anisotropy in Case II at time  $t = 0.5$  with different  $\beta$ .

### 5.1 Results for the anisotropic surface diffusion

Here we provide convergence tests to show the quadratic convergence rate in space and linear convergence rate in time. To this end, the time step  $\tau$  is always chosen as  $\tau = h^2$  except it is state otherwise. The distance between two closed curves  $\Gamma_1, \Gamma_2$  is given by the manifold distance  $M(\Gamma_1, \Gamma_2)$  in [45] as

$$M(\Gamma_1, \Gamma_2) := 2|\Omega_1 \cup \Omega_2| - |\Omega_1| - |\Omega_2|, \quad (5.1)$$

where  $\Omega_1, \Omega_2$  are the interior regions of  $\Gamma_1, \Gamma_2$ , respectively, and  $|\Omega|$  denotes the area of  $\Omega$ . Let  $\Gamma^m$  be the numerical approximation of  $\Gamma^h(t = t_m := m\tau)$  with mesh size  $h$  and time step  $\tau$ , the numerical error is thus given as

$$e^h(t) \Big|_{t=t_m} := M(\Gamma^m, \Gamma(t_m)). \quad (5.2)$$

To numerically test the energy stability, area conservation and good mesh quality, we introduce the following indicators: the normalized energy  $\frac{W^h(t)}{W^h(0)} \Big|_{t=t_m} := \frac{W^m}{W^0}$ , the normalized area loss and the weighted mesh ratio

$$\frac{\Delta A^h(t)}{A^h(0)} \Big|_{t=t_m} := \frac{A^m - A^0}{A^0}, \quad R_\gamma^h(t) \Big|_{t=t_m} := \frac{\max_{1 \leq j \leq N} |\mathbf{h}_j^m| \gamma(\mathbf{n}_j^m)}{\min_{1 \leq j \leq N} |\mathbf{h}_j^m| \gamma(\mathbf{n}_j^m)}. \quad (5.3)$$

In the following numerical tests, the initial curve  $\Gamma_0$  is given as an ellipse with length 4 and width 1. The exact solution  $\Gamma(t)$  is approximated by choosing  $k(\mathbf{n}) = k_0(\mathbf{n})$  with  $h = 2^{-8}$  and  $\tau = 2^{-16}$  in (2.31). Here are two typical anisotropic surface energies to be taken in our simulations:

- Case I:  $\gamma(\mathbf{n}) = \sqrt{\left(\frac{5}{2} + \frac{3}{2} \text{sgn}(n_1)\right) n_1^2 + n_2^2}$  [19];

- Case II:  $\gamma(\mathbf{n}) = 1 + \beta \cos(3\theta)$  with  $\mathbf{n} = (\sin\theta, -\cos\theta)^T$  and  $|\beta| < 1$  [29]. It is weakly anisotropic when  $|\beta| < \frac{1}{8}$ , and otherwise it is strongly anisotropic.

Fig. 5.1 presents the convergence rates of the proposed SP-PFEM (2.31) at different times and with different anisotropic strengths  $\beta$  under a fixed time  $t = 0.5$ . It is apparent from this figure that the second-order convergence in space is independent of anisotropies and computation times, which indicates the convergence rate is very robust.

The time evolution of the normalized energy  $\frac{W^h(t)}{W^h(0)}$  with different  $h$ , the normalized area loss  $\frac{\Delta A^h(t)}{A^h(0)}$  and the number of Newton iterations with  $h = 2^{-7}$ , and the weighted mesh quality  $R_\gamma^h(t)$  with different  $h$  are summarised in Figs. 5.2-5.4, respectively.

It can be seen from Figs. 5.2-5.4 that

- (i) The normalized energy is monotonically decreasing when the surface energy satisfies the energy stable condition (2.37) (cf. Fig. 5.2);
- (ii) The normalized area loss is at  $10^{-15}$  which is almost at the same order as the round-off error (cf. Fig. 5.2), which confirms the area conservation in practical simulations;
- (iii) Interestingly, the numbers of iterations in Newton's method are initially 2 and finally 1 (cf. Fig. 5.3). This finding suggests that although the proposed SP-PFEM (2.31) is full-implicit, but it can be solved very efficiently with a few iterations;
- (iv) In Fig. 5.4 there is a clear trend of convergence of the weighted mesh ratio  $R_\gamma^h$ . Moreover, in contrast to the symmetrized SP-PFEM for symmetric  $\gamma(\mathbf{n})$  in [3],  $R_\gamma^h$  keeps small even with the strongly anisotropy  $\gamma(\mathbf{n}) = 1 + \frac{1}{3} \cos 3\theta$ .

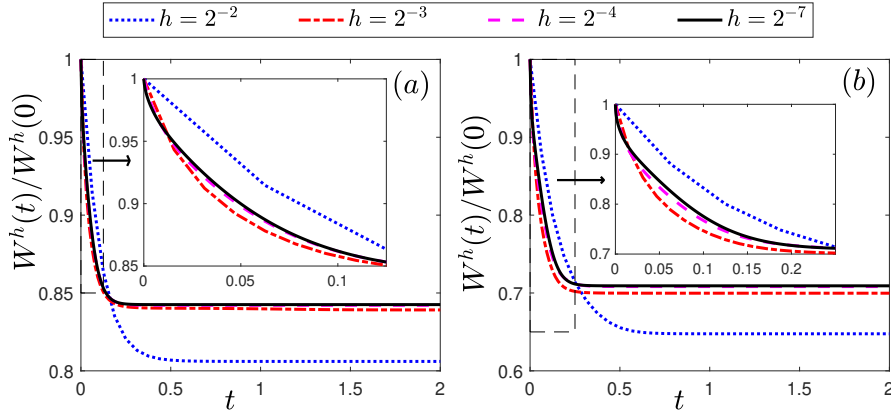


Fig. 5.2: Normalized energy of the SP-PFEM (2.31) with  $k(\mathbf{n}) = k_0(\mathbf{n})$  and different  $h$  for: (a) anisotropy in Case I; (b) anisotropy in Case II with  $\beta = \frac{1}{3}$ .

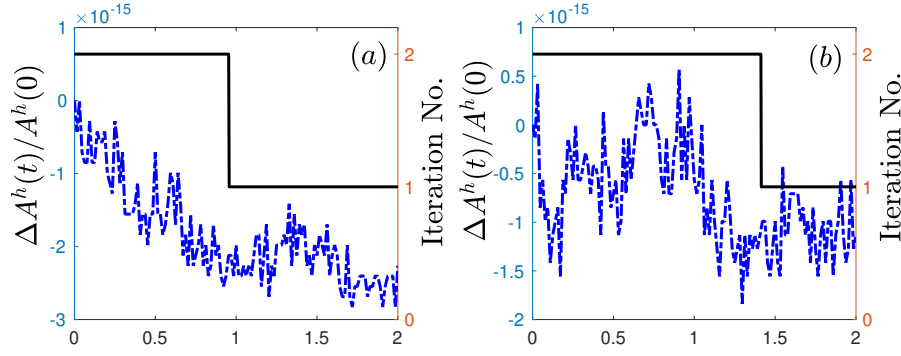


Fig. 5.3: Normalized area loss (blue dashed line) and iteration number (black line) of the SP-PFEM (2.31) with  $k(\mathbf{n}) = k_0(\mathbf{n})$  and  $h = 2^{-7}$ ,  $\tau = h^2$  for: (a) anisotropy in Case I; (b) anisotropy in Case II with  $\beta = \frac{1}{3}$ .

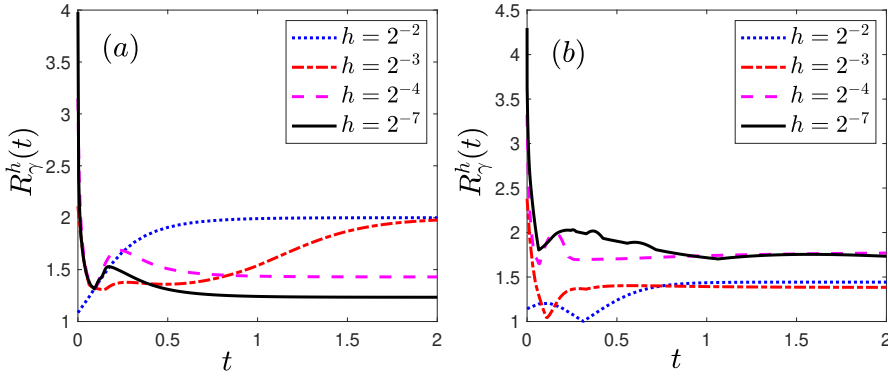


Fig. 5.4: Weighted mesh ratio of the SP-PFEM (2.31) with  $k(\mathbf{n}) = k_0(\mathbf{n})$  and different  $h$  for: (a) anisotropy in Case I; (b) anisotropy in Case II with  $\beta = \frac{1}{3}$ .

## 5.2 Application for morphological evolutions

Finally, we apply the proposed SP-PFEMs to simulate the morphological evolutions driven by the three anisotropic geometric flows. Fig 5.5 plots the morphological evolutions of anisotropic surface diffusion for the four different anisotropic energies: (a) anisotropy in case I; (b)-(d) anisotropies in case II with  $\beta = 1/9, 1/7, 1/3$ , respectively. Fig 5.6 and Fig 5.7 depict the anisotropic surface diffusion, area-conserved anisotropic curvature flow, and anisotropic curvature flow at different times with anisotropy in case I and in case II with  $\beta = 1/3$ , respectively.

As shown in Fig. 5.5 (b)-(d), the edges emerge during the evolution and corners become sharper as the strength  $\beta$  increases. In contrast, there are no edges or corners in the morphological evolutions with anisotropy in Case I. This suggests that even if it is not a  $C^2$ -function, it is more like weak anisotropy! From Fig. 5.6-5.7, we can see that

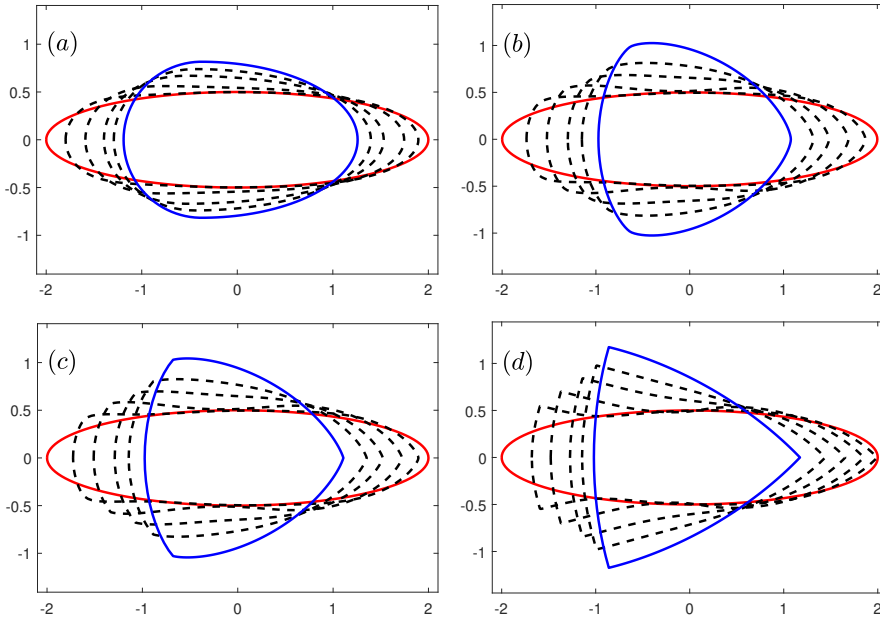


Fig. 5.5: Morphological evolutions of a  $4 \times 1$  ellipse under anisotropic surface diffusion with four different anisotropic energies: (a) anisotropy in Case I; (b)-(d) anisotropies in case II with  $\beta = 1/9, 1/7, 1/3$ , respectively. The red and blue lines represent the initial curve and the numerical equilibrium, respectively; and the black dashed lines represent the intermediate curves. The mesh size and time step are taken as  $h = 2^{-7}, \tau = h^2$ .

the anisotropic surface diffusion and the area-conserved anisotropic curvature flow have the same equilibriums in shapes, while they have different dynamics, i.e., the equilibriums are different in positions, and the anisotropic surface diffusion evolves faster than the area-conserved anisotropic curvature flow.

## 6 Conclusions

By introducing a novel surface energy matrix  $\mathbf{G}_k(\mathbf{n})$  depending on the anisotropic surface energy  $\gamma(\mathbf{n})$  and the Cahn-Hoffman  $\xi$ -vector as well as a nonnegative stabilizing function  $k(\mathbf{n})$ , we proposed conservative geometric partial differential equations for several geometric flows with anisotropic surface energy  $\gamma(\mathbf{n})$ . We derived their weak formulations and applied PFEM to get their full discretizations. Then we proved these PFEMs are structure-preserving under a very mild condition on  $\gamma(\mathbf{n})$  with proper choice of the stabilizing function  $k(\mathbf{n})$ . Though our surface energy matrix  $\mathbf{G}_k(\mathbf{n})$  is no longer symmetric, our experiments had shown a robust second-order convergence rate in space and linear convergence rate in time and unconditional energy stability. Specifically, the mesh quality of the proposed SP-PFEM, i.e. the weighted mesh ratio is much smaller, is much better than that in the symmetrized SP-PFEM proposed

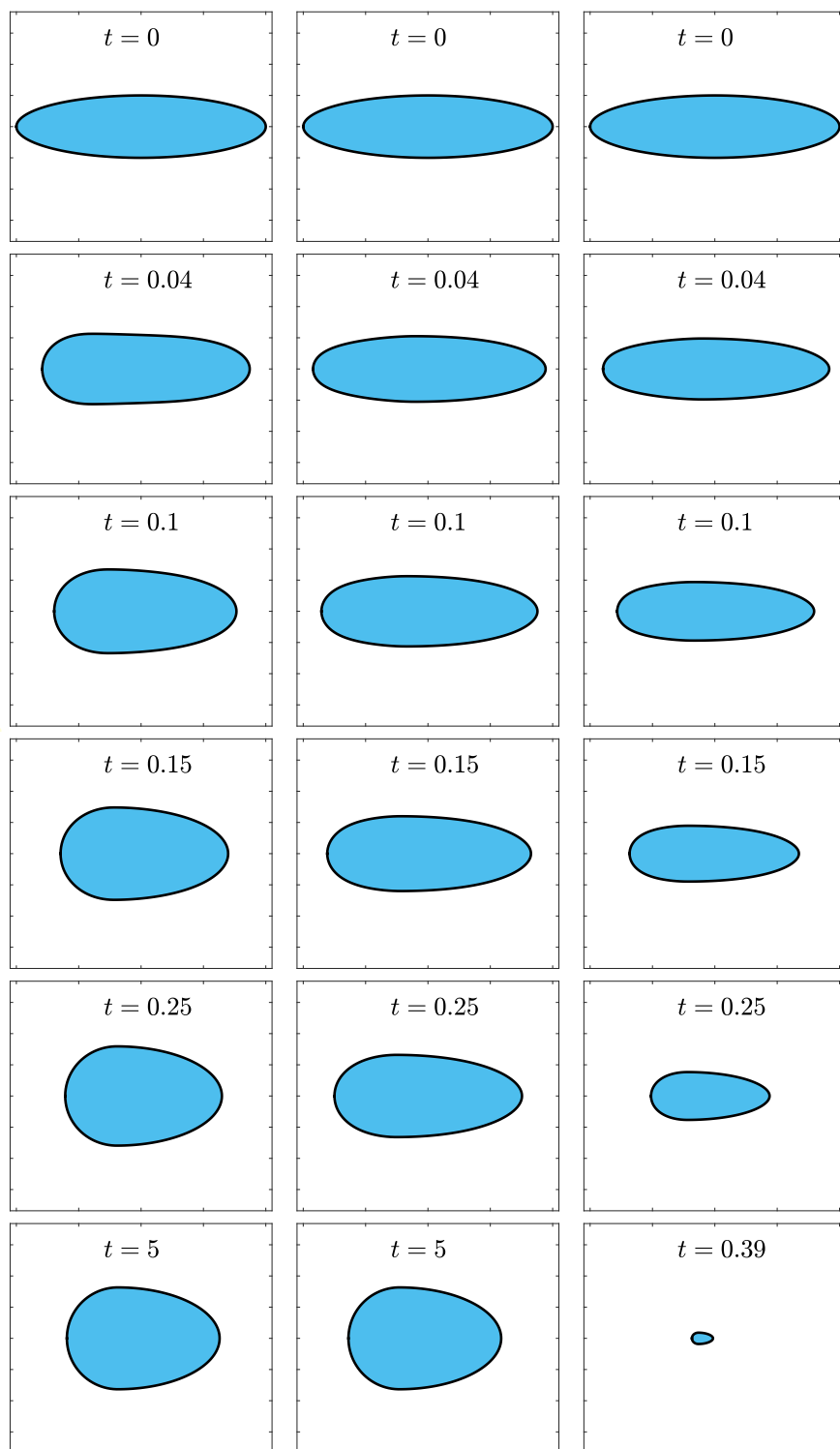


Fig. 5.6: Morphological evolutions of a  $4 \times 1$  ellipse under anisotropic surface diffusion (left column), area-conserved anisotropic curvature flow (middle column) and anisotropic curvature flow (right column) with the anisotropic surface energy in Case I at different times. The evolving curves and their enclosed regions are colored by blue and black. The mesh size and time step are taken as  $h = 2^{-7}$ ,  $\tau = 0.001$ .

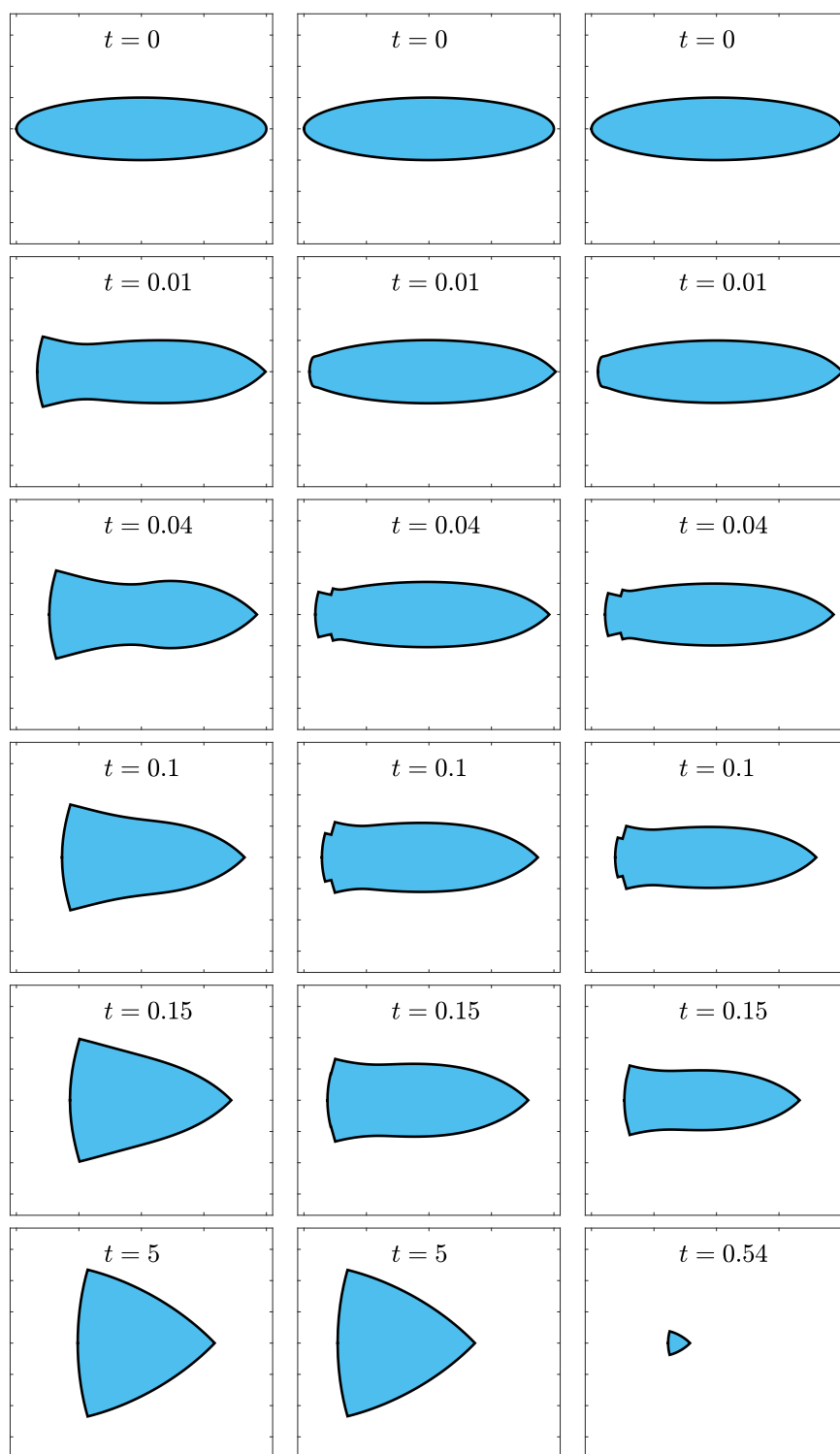


Fig. 5.7: Morphological evolutions of a  $4 \times 1$  ellipse under anisotropic surface diffusion (left column), area-conserved anisotropic curvature flow (middle column) and anisotropic curvature flow (right column) with the anisotropic surface energy in Case II with  $\beta = 1/3$  at different times. The evolving curves and their enclosed regions are colored by blue and black. The mesh size and time step are taken as  $h = 2^{-7}$ ,  $\tau = 0.001$ .

recently for anisotropic surface diffusion with a symmetric surface energy [3, 5]. Moreover, our SP-PFEMs work well for the piecewise  $C^2$  anisotropy, which is a significant achievement compared with other PFEMs. In the future, we will generalize the surface energy matrix  $\mathbf{G}_k(\mathbf{n})$  to three dimensions (3D) and propose efficient and accurate SP-PFEM for anisotropic geometric flows in 3D.

## References

1. B. Andrews, Volume-preserving anisotropic mean curvature flow, *Indiana Univ. Math. J.*, (2001), pp. 783-827.
2. W. Bao, H. Garcke, R. Nürnberg, and Q. Zhao, Volume-preserving parametric finite element methods for axisymmetric geometric evolution equations, *J. Comput. Phys.*, 460 (2022), pp. 111180.
3. W. Bao, W. Jiang, and Y. Li, A symmetrized parametric finite element method for anisotropic surface diffusion of closed curves, *SIAM J. Numer. Anal.*, to appear (arXiv preprint arXiv:2112.00508), (2021).
4. W. Bao, W. Jiang, Y. Wang, and Q. Zhao, A parametric finite element method for solid-state dewetting problems with anisotropic surface energies, *J. Comput. Phys.*, 330 (2017), pp. 380-400.
5. W. Bao and Y. Li, A symmetrized parametric finite element method for anisotropic surface diffusion in 3D, arXiv preprint arXiv:2206.01883, (2022).
6. W. Bao and Q. Zhao, An energy-stable parametric finite element method for simulating solid-state dewetting problems in three dimensions, *J. Comput. Math.*, to appear (arXiv preprint arXiv:2012.11404), (2020).
7. W. Bao and Q. Zhao, A structure-preserving parametric finite element method for surface diffusion, *SIAM J. Numer. Anal.*, 59 (2021), pp. 2775-2799.
8. J. W. Barrett, H. Garcke, and R. Nürnberg, A parametric finite element method for fourth order geometric evolution equations, *J. Comput. Phys.*, 222 (2007), pp. 441-467.
9. J. W. Barrett, H. Garcke, and R. Nürnberg, Numerical approximation of anisotropic geometric evolution equations in the plane, *IMA J. Numer. Anal.*, 28 (2008), pp. 292-330.
10. J. W. Barrett, H. Garcke, and R. Nürnberg, On the parametric finite element approximation of evolving hypersurfaces in  $\mathbb{R}^3$ , *J. Comput. Phys.*, 227 (2008), pp. 1-44.
11. J. W. Barrett, H. Garcke, and R. Nürnberg, A variational formulation of anisotropic geometric evolution equations in higher dimensions, *Numer. Math.*, 109 (2008), pp. 1-44.
12. J. W. Barrett, H. Garcke, and R. Nürnberg, A variational formulation of anisotropic geometric evolution equations in higher dimensions, *Eur. J. Appl. Math.*, 21 (2010), pp. 519-556.
13. J. W. Barrett, H. Garcke, and R. Nürnberg, Parametric finite element approximations of curvature-driven interface evolutions, in *Handb. Numer. Anal.*, 21 (2020), pp. 275-423.
14. J. Cahn, Stability, microstructural evolution, grain growth, and coarsening in a two-dimensional two-phase microstructure, *Acta Metall. Mater.*, 39 (1991), pp. 2189-2199.
15. J. W. Cahn and J. E. Taylor, Overview no. 113 surface motion by surface diffusion, *Acta Metall. Mater.*, 42 (1994), pp. 1045-1063.
16. W. C. Carter, A. Roosen, J. W. Cahn, and J. E. Taylor, Shape evolution by surface diffusion and surface attachment limited kinetics on completely faceted surfaces, *Acta Metall. Mater.*, 43 (1995), pp. 4309-4323.
17. Y. Chen, Y. Giga, and S. Goto, Uniqueness and existence of viscosity solutions of generalized mean curvature flow equations, in *Fundamental Contributions to the Continuum Theory of Evolving Phase Interfaces in Solids*, Springer, 1999, pp. 375-412.
18. U. Clarenz, U. Diewald, and M. Rumpf, Anisotropic geometric diffusion in surface processing, *IEEE Vis. 2000*, 2000.
19. K. Deckelnick, G. Dziuk, and C. M. Elliott, Computation of geometric partial differential equations and mean curvature flow, *Acta Numer.*, 14 (2005), pp. 139-232.
20. K. Deckelnick, G. Dziuk, and C. M. Elliott, Fully discrete finite element approximation for anisotropic surface diffusion of graphs, *SIAM J. Numer. Anal.*, 43 (2005), pp. 1112-1138.
21. I. C. Dolcetta, S. F. Vita, and R. March, Area-preserving curve-shortening flows: from phase separation to image processing, *IFB*, (2002), pp. 325-343.



22. P. Du, M. Khennar, and H. Wong, A tangent-plane marker-particle method for the computation of three-dimensional solid surfaces evolving by surface diffusion on a substrate, *J. Comput. Phys.*, 229 (2010), pp. 813-827.
23. Q. Du and X. Feng, The phase field method for geometric moving interfaces and their numerical approximations, in *Handb. Numer. Anal.*, 21 (2020), pp. 425-508.
24. I. Fonseca, A. Pratelli and B. Zwicknagl, Shapes of epitaxially grown quantum dots, *Arch. Ration. Mech. Anal.*, 214 (2014), pp. 359-401.
25. P. M. Girao and R. V. Kohn, The crystalline algorithm for computing motion by curvature, in *Variational Methods for Discontinuous Structures*, Springer, 1996, pp. 7-18.
26. M. E. Gurtin and M. E. Jabbur, Interface evolution in three dimensions with curvature-dependent energy and surface diffusion: interface-controlled evolution, phase transitions, epitaxial growth of elastic films, *Arch. Ration. Mech. Anal.*, 163 (2002), pp. 171-208.
27. D. W. Hoffman and J. W. Cahn, A vector thermodynamics for anisotropic surfaces: I. fundamentals and application to plane surface junctions, *Surf. Sci.*, 31 (1972), pp. 368-388.
28. W. Jiang, W. Bao, C. V. Thompson, and D. J. Srolovitz, Phase field approach for simulating solid-state dewetting problems, *Acta Mater.*, 60 (2012), pp. 5578-5592.
29. W. Jiang, Y. Wang, Q. Zhao, D. J. Srolovitz, and W. Bao, Solid-state dewetting and island morphologies in strongly anisotropic materials, *Scr. Mater.*, 115 (2016), pp. 123-127.
30. W. Jiang and Q. Zhao, Sharp-interface approach for simulating solid-state dewetting in two dimensions: A Cahn-Hoffman  $\xi$ -vector formulation, *Phys. D*, 390 (2019), pp. 69-83.
31. B. Kovaács, B. Li, and C. Lubich, A convergent evolving finite element algorithm for mean curvature flow of closed surfaces, *Numer. Math.*, 143 (2019), pp. 797-853.
32. Y. Li and W. Bao, An energy-stable parametric finite element method for anisotropic surface diffusion, *J. Comput. Phys.*, 446 (2021), p. 110658.
33. W. J. Niessen, B. M. Romeny, L. M. Florack, and M. A. Viergever, A general framework for geometry-driven evolution equations, *Int. J. Comput. Vis.*, 21 (1997), pp. 187-205.
34. S. Randolph, J. Fowlkes, A. Melechko, K. Klein, H. Meyer, M. Simpson, and P. Rack, Controlling thin film structure for the dewetting of catalyst nanoparticle arrays for subsequent carbon nanofiber growth, *Nanotech.*, 18 (2007), p. 465354.
35. H. Shen, S. Nutt, and D. Hull, Direct observation and measurement of fiber architecture in short fiber-polymer composite foam through micro-CT imaging, *Compos. Sci. Technol.*, 64 (2004), pp. 2113-2120.
36. A. P. Sutton and R. W. Balluffi, *Interfaces in crystalline materials*, Clarendon Press, 1995.
37. J. E. Taylor, Mean curvature and weighted mean curvature, *Acta Metall. Mater.*, 40 (1992), pp. 1475-1485.
38. J. E. Taylor, J. W. Cahn, and C. A. Handwerker, Overview no. 98 i—geometric models of crystal growth, *Acta Metall. Mater.*, 40 (1992), pp. 1443-1474.
39. C. V. Thompson, Solid-state dewetting of thin films, *Annu. Rev. Mater. Res.*, 42 (2012), pp. 399-434.
40. Y. Wang, W. Jiang, W. Bao, and D. J. Srolovitz, Sharp interface model for solid-state dewetting problems with weakly anisotropic surface energies, *Phys. Rev. B*, 91 (2015), p. 045303.
41. A. Wheeler, Cahn-Hoffman  $\xi$ -vector and its relation to diffuse interface models of phase transitions, *J. Stat. Phys.*, 95 (1999), pp. 1245-1280.
42. H. Wong, P. Voorhees, M. Miksis, and S. Davis, Periodic mass shedding of a retracting solid film step, *Acta Mater.*, 48 (2000), pp. 1719-1728.
43. Y. Xu and C. Shu, Local discontinuous Galerkin method for surface diffusion and Willmore flow of graphs, *J. Sci. Comput.*, 40 (2009), pp. 375-390.
44. J. Ye and C. V. Thompson, Mechanisms of complex morphological evolution during solid-state dewetting of single-crystal nickel thin films, *Appl. Phys. Lett.*, 97 (2010), p. 071904.
45. Q. Zhao, W. Jiang, and W. Bao, An energy-stable parametric finite element method for simulating solid-state dewetting, *IMA J. Num. Anal.*, 41 (2021), pp. 2026-2055.